M.T. Klein and P.S. Virk
Department of Chemical Engineering
Massachusetts Institute of Technology
Cambridge, MA 02139

We hypothesize that during pyrolysis of lignites, the primary evolution of gas occurs from lignin-related residues in the coal. Likely pathways for this primary gas release have been theoretically modelled by a set of thermally-allowed pericyclic reactions that respectively lead to each of methane, carbon monoxide, carbon dioxide, and water products from substrates containing lignoid moieties. The model pathways for methane formation can be experimentally examined by pyrolysis of a series of methoxy-benzenes, e.g., anisole MeO-⬡, guaiacol MeO-⬡(HO), and iso-eugenol MeO-⬡(HO)-⟍.

Experiments over the temperature range 200-500 C in batch tubing-bomb reactors equipped for gas and liquid product analyses showed that guaiacol was appreciably more reactive than anisole, fractional conversions of these substrates at 420 C and 120 s being respectively 0.083 and 0.0022. The former pyrolysis was essentially first order both in guaicol disappearance as well as in methane gas appearance and yielded Arrhenius parameters ($\log_{10}A$ s^{-1}, E^* kcal/mol) = (11.5, 45.8). These data accord with the hypothesis that methane release from guaiacyl moieties occurs by a concerted molecular group-transfer reaction.

EFFECTS OF COAL STRUCTURE AND PROCESSING CONDITIONS ON ORGANIC EFFLUENTS FROM SLAGGING FIXED-BED GASIFICATION

Jacquelyn K. Olson and Harold H. Schobert

Grand Forks Energy Technology Center
U.S. Department of Energy
Grand Forks, ND 58202

INTRODUCTION

Slagging fixed-bed gasification of low-rank coals is being investigated at the Grand Forks Energy Technology Center. In support of environmental and waste treatment studies, research is underway to determine the effect of process parameters on effluent production and composition.

The GFETC gasifier is a 1 ton/hour, pilot plant unit. The coal feed moves slowly down a shaft and is reacted with an oxygen-steam mixture injected through four tuyeres into the hearth. The product gas exits the gasifier at the top of the shaft. Operating parameters that may vary from test to test are pressure, 100 to 400 psig; oxygen/ steam molar ratio, 0.9 to 1.1; and oxygen feed rate, 4000 to 6000 scfh. Detailed information on the GFETC pilot plant studies has been published previously (1-3).

Tar, oils, water vapor and coal particles are removed from the exiting raw gas stream in a spray washer. The liquids that accumulate in the spray washer are sampled periodically. A recent publication (4) describes spray washer sampling procedures. Samples considered in this report were collected at the end of the test.

An inherent problem in the analysis of effluents from coal conversion processes is the complexity of the mixtures. Several schemes have been suggested for the analysis and environmental assessment of coal gasification effluents. The methodology defined by the EPA-IERL/RTP Procedure Manual: Level 1 Environmental Assessment (5) was applied to the analysis of spraywasher samples. Effluent samples produced by gasification of three coals at a range of conditions were used for this study.

EXPERIMENTAL

Figure 1 is the flow diagram of the separations and analyses performed on the tar and liquor samples.

Simulated distillation was obtained by FID gas chromatography using 3% OV-17, 1/8" x 4' ss columns. The temperature was programmed from 50 to 300°C at 10°/min. ASTM standard D2887 was used to establish boiling point ranges. The extracted organics were separated using gradient elution liquid chromatography. Silica gel adsorbent was used. Table 1 shows the solvent sequence for the procedure.

FIGURE 1. Analytical Flow Diagram for Spraywasher Tar and Liquor

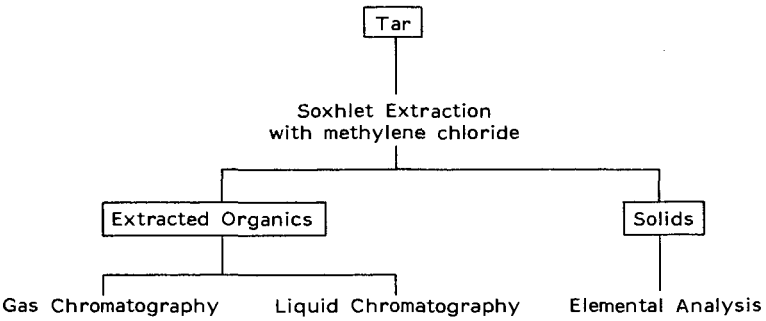

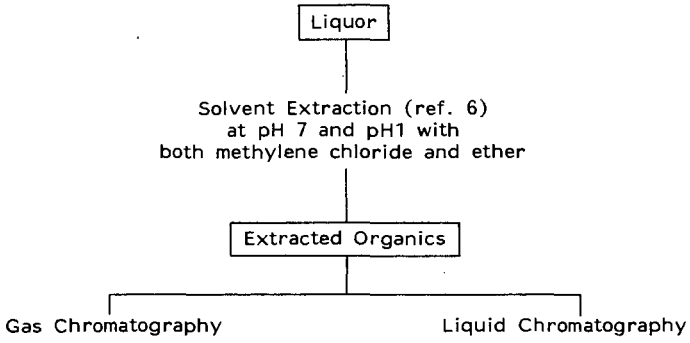

TABLE 1. Solvent Series for LC Separations

Fraction	Solvent Composition
1	Pentane
2	20% methylene chloride in pentane
3	50% methylene chloride in pentane
4	Methylene chloride
5	5% methanol in methylene chloride
6	20% methanol in methylene chloride
7	50% methanol in methylene chloride
8	Methanol

Instruments used in this study were an AEI MS-30* mass spectrometer, Perkin-Elmer 240 elemental analyzer, Leco sulfur analyzer, Varian 2400 gas chromatograph, and Perkin-Elmer 283 infrared spectrophotometer.

RESULTS

End-of-run tar and liquor samples produced from five gasification tests were obtained for this study. The summary of coals and operating parameters for these tests is shown in Table 2.

TABLE 2. Summary of Coals and Operating Parameters

Run No.	Coal/Rank	Operating Pressure (psig)	Oxygen Feed Rate (scfh)	Oxygen-Steam Molar Ratio
RA-40	Indian Head Lignite	200	4000	1.0
RA-52	Indian Head Lignite	300	6000	1.0
RA-37	Indian Head Lignite	400	6000	1.0
RA-45	Rosebud Subbituminous	200	4000	1.1
RA-58	Gascoyne Lignite	300	6000	1.1

Tar

The as-received tar contained 28 to 35% extractable organic material, 0.4 to 2.0% solids (entrained coal particles) and 63 to 71% water. The gas chromatographic analysis of the organic extracts is shown in Table 3.

TABLE 3. GC Analysis of Organics Extracted from Tar

Range	BP(°C)	% of Extract				
		RA-40	RA-52	RA-37	RA-45	RA-58
C_7	90 to 110	0.4	0.1	0	0	1.5
C_8	110 to 140	0.8	0.2	0.1	0	2.4
C_9	140 to 160	0.1	0.6	0.2	0.2	3.3
C_{10}	160 to 180	1.1	0.6	0.3	0.8	6.8
C_{11}	180 to 200	2.5	0.8	0.6	1.4	5.0
C_{12}	200 to 220	10.0	11.6	11.8	7.3	20.0
$>C_{12}$	> 220	85.1	86.1	87.0	90.3	61.0

* Identification of specific brands or models is done to facilitate understanding and does not constitute or imply endorsement by the Department of Energy.

The distribution of compound classes in the liquid chromatography separations was determined by low voltage mass spectrometry and confirmed by infrared spectroscopy. Fraction 1 consists of paraffins and olefins, mostly branched. Fractions 2 and 3 consist primarily of naphthalene, C_1 and C_2 naphthalenes, and C_1 biphenyl or C_1 acenaphthene. Fractions 4 and 5 consist primarily of C_1 acenaphthylene or C_1 fluorene, phenanthrene, anthracene, C_1 and C_2 phenanthrene, C_1 and C_2 anthracene, fluoranthene, pyrene, and C_1 pyrene. Fractions 6 and 7 consist primarily of C_1 and C_3 indoles, naphthol, C_1 and C_2 napthols, carbazole, C_2, C_3, and C_4 pyridines, phenol, and C_1, C_2, and C_3 phenols. No specific assignments were made to the compounds in fraction 8. The results of the liquid chromatography separations of the organics extracted from the tar are shown in Table 4.

TABLE 4. LC Analysis of Organics Extracted from Tar

Fraction(s)	% of Extract				
	RA-40	RA-52	RA-37	RA-45	RA-58
1	10.3	11.4	9.0	12.0	13.0
2,3,4	32.3	29.9	27.8	33.9	41.0
5,6,7	51.8	57.4	61.7	48.6	45.3
8	5.6	1.3	1.5	5.5	0.7

Liquor

Runs RA-40, RA-45, and RA-58 liquor yielded from 1200 to 2050 ppm solvent extractable organics. It is unlikely that the majority of organics were extracted since the total organic carbon for these liquors ranges from 6550 to 7800 ppm. The gas chromatography analysis of the extracted organics is shown in Table 5.

TABLE 5. GC Analysis of Organics Extracted from Liquor

Range	BP(°C)	% of Extract		
		RA-40	RA-45	RA-58
C_7	90 to 110	0	0	0.4
C_8	110 to 140	0	0	0.7
C_9	140 to 160	0	0	1.3
C_{10}	160 to 180	0	0	2.5
C_{11}	180 to 200	0.1	0	3.2
C_{12}	200 to 220	16.1	11.5	7.8
$>C_{12}$	> 220	83.9	88.5	84.0

The liquid chromatography separations of the organic extract were not useful in defining specific classes of compounds. There was a considerable amount of overlap in the compounds found in fractions 5 through 8. These fractions consist primarily of C_4 and C_5 benzenes, C_1 and C_2 pyridines, C_2 and C_3 phenols, quinolines, naphthols, phenanthrene, anthracene, binaphthyl, and thiophenes. These assignments were made by mass spectrometry and infrared spectroscopy. The liquid chromatography analysis of the extracted organics is shown in Table 6.

TABLE 6. LC Analysis of Organics Extracted from Liquor

Fraction(s)	% of Extract		
	RA-40	RA-45	RA-58
1	0	0	1.6
2,3,4	0.4	0.4	8.3
5,6,7	80.8	89.2	83.0
8	18.8	10.2	7.1

Tar Solids

The solids were found to contain a higher percentage of mineral matter than the original coal feed. The relative proportion of nitrogen and sulfur was also higher in the solids. For RA-45, the coal feed contained 0.85% nitrogen and 1.81% sulfur; the solids contained 3.32% nitrogen and 2.42% sulfur. Table 7 shows the ultimate analyses of the tar solids and the feed coals.

TABLE 7. Comparison of Tar Solids with Feed Coal

	RA-40		RA-45		RA-58	
	feed coal	tar solids	feed coal	tar solids	feed coal	tar solids
Ultimate Analysis*, pct						
C	64.42	65.34	64.23	58.99	62.14	63.05
H	4.35	4.11	4.31	1.49	4.39	3.05
N	0.85	3.32	1.01	1.46	0.84	1.21
S	1.81	2.42	2.05	3.59	1.42	1.74
O(by diff)	18.23	13.77	13.06	0.66	18.06	10.22
Ash	10.34	11.04	15.34	33.81	13.15	20.73

*moisture-free basis

DISCUSSION

Tar Characterization

The variation observed in the amount of organic material extracted from the tar phase is consistent with experimental error in sampling. The procedure for obtaining tar samples has been described previously (4). The phase separation of tar from liquor depends on operator judgement in observing the interface between two darkly colored phases. Tar extraction data for runs 40, 45, and 58 shows a relative standard deviation of 6.01% for the amount of water. Three other runs made with Indian Head lignite at 200 psi and 4000 scfh oxygen rate showed a relative standard deviation of 6.47% for water content. Thus the variation between samples of different coals tested at different gasification conditions is nearly identical to that for replicate runs with the same coal.

The boiling point distribution of the tar extract shows distinct differences when comparing tars obtained from different coals gasified under same conditions. For example, a comparison of Rosebud and Indian Head gasified at 200 psi shows the tar from Indian Head to be comprised of more lower boiling materials. The cumulative boiling point distribution shows that 46% of Indian Head tar has distilled by 254°C and 87% by 343°, while the comparable figures for Rosebud tar are 34% and 76%. Of these two coals, Indian Head contains the greater amount of volatile

matter on an maf basis. A similar effect was observed for tars from gasification of Gascoyne and Indian Head lignites at 300 psi: Gascoyne contains a greater amount of volatile matter and produces more low boiling compounds in the tar.

A comparison of the boiling point distributions of tars produced from gasification of Indian Head lignite at different pressures shows that the effect of increasing gasification pressure is to shift the boiling point distribution downward. For example, the temperatures at which 75% of the tar has distilled drop from 316°C for tar produced at 200 psi, to 287° for 300 psi, and to 271° for tar produced at 400 psi. The fraction corresponding to phenol (180-200°C) decreases with increasing gasification pressure, as shown previously (7) for a high-pressure, low-temperature carbonization process in the SFBG.

The amounts of the fractions obtained in the liquid chromatographic separations of the tar were correlated with gasification conditions and coal composition. The treatment used followed the fractional factorial analysis procedures given by Lipson and Sheth (8). Since the absolute numerical values of the factors vary over several orders of magnitude -from thousands of scfm for oxygen feed rates to one or two percentage units for coal nitrogen and sulfur - comparisons were made on the basis of percentage changes in each factor.

The amounts of fractions 1 (paraffins and olefins), 2-4 (aromatics), and 5-7 (polar compounds) depend most heavily on the maf carbon content of the coals. Both the paraffins and olefins and the aromatics show a direct correlation with maf carbon, while the polar compounds vary inversely. These results demonstrate that as more carbon is added to the molecular framework of the coal proportionately fewer oxygen or nitrogen functional groups will be present; hence as the coal undergoes pyrolysis or hydrocracking in the carbonization zone of the SFBG (9) relatively fewer polar species will be formed. Correlation of the amounts of one LC fraction vs. another show that the paraffins and olefins are directly proportional to the aromatics, but that both the paraffin-olefin and the aromatic fractions vary inversely with the polar fraction.

When the effect of maf carbon content in the coal is removed statistically (8), no other factors were found to influence the amount of the paraffin-olefin fraction. The amount of the aromatic fraction, corrected for the effect of carbon, shows a direct correlation with the amount of hydrogen in the product gas. A recent publication (10) describing the detailed mass spectroscopic analysis of SFBG tars also demonstrated such a correlation for the concentrations of many of the aromatic compounds. The amount of the polar fraction showed no other correlations above the 80% confidence limit.

With respect to the amount of the very polar fraction (fraction 8) no factors were found to display both a large slope and greater than 80% confidence correlation.

Liquor Characterization

The amount of organic material extractable from the liquor accounted for only 18 to 28% of the total organic carbon content of the samples. The amount of extractable material shows an inverse correlation with the maf oxygen content of the coal. As the oxygen content of the coal increases, more compounds with polar functional groups should appear in the organic effluents; these compounds should dissolve in the liquor and in turn be resistant to extraction into relatively non-polar solvents. The amount of extractable organic material when added to the "phenols" as determined by gas chromatographic analysis of filtered liquor (11) agrees well with the total organic carbon content. For example; in the liquor produced during gasification of Rosebud coal, phenols accounted for 75.9% of the TOC and the extractable organics, 28.3%.

The boiling point distributions of liquor organic extracts from gasification of Indian Head (RA-40), Rosebud, and Gascoyne are similar. The most appreciable difference is that the extract from liquor produced in gasification of Gascoyne lignite is the only one of the three samples containing material boiling below 196°C. The liquid chromatographic separation of the extract from Gascoyne liquor was the only one showing material in the paraffin-olefin and aromatic fractions.

A correlation of the amounts of fractions in the liquid chromatographic separations with gasification conditions and coal composition was performed in the same manner as for the tar extracts. Only the polar and polar fractions were considered, and only the three samples from runs 40, 45, and 58 were used.

The major factor affecting the amount of both fractions is the maf carbon content of the coal. The polar fraction correlates directly with maf carbon; the very polar fraction thus shows an inverse correlation, since these two fractions account for 90 to 99% of the total material in the liquor or organic extract.

Solids Characterization

A comparison of the ultimate analysis of solids recovered from the tar samples with that of the respective coals shows that in all cases the tar solids contain greater amounts of nitrogen and sulfur than the coals. Since these solids are coal particles which did not descend through the entire SFBG shaft to the gasification/combustion zone this finding suggests that compounds of carbon, hydrogen, and oxygen are more easily formed in the carbonization zone whereas nitrogen and sulfur linkages are more resistant to cleavage or reaction.

The ash in the solids recovered from tar from Indian Head gasification shows an enrichment on sodium, magnesium, sulfur, and iron when compared with the ash of the feed coal. As-yet unpublished work on the volatization of ash components in the SFBG gasification/combustion zone has shown that sodium, magnesium, and sulfur are the most volatile of the ash components.

In the case of both lignites, the mole fractions of the principal basic oxides essentially balance those of the silica and sulfur trioxide. The inorganic solids are therefore a mixture of alkali and alkaline earth silicates and sulfates. The ash from the solids recovered from Rosebud tar does not display such a balance. A petrographic classification by the Niggli method (12) shows that free quartz should be present, suggesting that the inorganic solids in this case are a mixture of alkali and alkaline earth sulfates with quartz particles.

CONCLUSIONS

The carbon content of the coal plays the most predominant role in determining the relative amounts of compound types in the organic extracts from tar and liquor. An increase in maf carbon will increase the percentage of paraffins and olefins and aromatics in the tar and will increase the percentage of polar compounds in the liquor extract. The polar fraction in the tar extract decreases as maf carbon in the coal increases. The oxygen content of the coal correlates inversely with the amount of organic material extractable from the liquor. Since the carbon content of the coal is of great importance in determining the molecular framework, and since the oxygen is the major contributor to heteroatomic functional groups, these results show that the effluent composition is dependent upon the molecular structure of the coal. Other coal-specific characteristics of the SFBG effluents include the volatility of the tar and the nature of the inorganic materials exiting the gasifier in the raw gas.

Research on the development of detailed relationships between coal composition or structure and effluent composition is continuing. The results of this study indicate the desirability of testing a wide variety of coals in the SFBG to augment the data base on effluent characteristics.

References

1. Gronhovd, G. H., Harak, A. E., Fegley, M. M. and D. E. Severson. Slagging Fixed-Bed Gasification of North Dakota Lignite at Pressures to 400 Psig. U.S. Bureau of Mines Report of Investigations 7408 (1970).

2. Ellman, R. C., Johnson, B. C., and M. M. Fegley. Studies in Slagging Fixed-Bed Gasification at the Grand Forks Energy Technology Center. Tenth Synthetic Pipeline Gas Symposium, Chicago (1978).

3. Ellman, R. C., and E. A. Sondreal. Environmental Control Activities on Slagging Fixed-Bed Gasification at the Grand Forks Energy Technology Center. U.S. Department of Energy Environmental Control Symposium, Washington, D.C. (1978).

4. Paulson, L. E., Schobert, H. H., and R. C. Ellman. Sampling, Analysis, and Characterization of Effluents from the Grand Forks Energy Research Center Slagging Fixed-Bed Gasifier. Division of Fuel Chemistry Preprints, 23(2):107 (1978).

5. Hamersma, J. W., Reynolds, S. L., and R. F. Maddalone. IERL-RTP Procedures Manual: Level 1 Environmental Assessment. EPA-600/2-76-160a (1976).

6. Bombaugh, K. J. Analysis of Grab Samples from Fixed-Bed Coal Gasification Processes. EPA-600/7-77-141 (1977).

7. Schobert, H. H., Johnson, B. C., and M. M. Fegley. Carbonization Reactions in the Grand Forks Fixed-Bed Slagging Gasifier. Div. Fuel Chemistry Preprints 23 (3), 136 (1978).

8. Lipson, C., and N. J. Sheth. Statistical Design and Analysis of Engineering Experiments. McGraw-Hill Book Co., New York (1973).

9. Johnson, B. C., Schobert, H. H., and M. M. Fegley. The Grand Forks Slagging Gasifier. Coal Processing Technology, vol. IV. American Institute of Chemical Engineers, New York (1978).

10. Miller, D. J., Olson, J. K., and H. H. Schobert. Mass Spectroscopic Characterization of Tars from the Gasification of Low Rank Coals. Div. Fuel Chemistry Preprints, in press (1979).

11. ASTM. Annual Book of ASTM Standards - Part 31 - Water. American Society for Testing and Materials, Philadelphia (1978).

12. Barth, T. F. W. Theoretical Petrology. John Wiley and Sons, New York (1962).

CATALYSIS OF LIGNITE CHAR GASIFICATION BY VARIOUS EXCHANGED CATIONS -- DEPENDENCE OF ACTIVITY ON REACTIVE ATMOSPHERE

P. L. Walker, Jr., O. P. Mahajan* and M. Komatsu

Department of Materials Science and Engineering
The Pennsylvania State University
University Park, PA 16802

INTRODUCTION

We have previously reported reactivities of a vast spectrum of coal-derived chars in air (1), CO_2 (2), steam (3) and H_2 (4). In oxidizing atmospheres, char reactivity decreases with increase in the rank of the parent coal. In contrast, char reactivity in H_2 shows little dependence on rank of the coal precursor.

Because of the large reserves of lignites and subbituminous coals in the United States, they are potentially of importance in coal conversion processes. These coals contain significant amounts of carboxylic acid groups, where a fraction of the H^+ ions have been exchanged by different cations such as Na^+, K^+, and Ca^{++}, as a result of extended contact with ground water containing different salts. The higher reactivity of lignite and sub-bituminous coal chars in oxidizing atmospheres is thought to be due, at least in part, to the presence of exchangeable metal cations. Therefore, it is desirable to study the possible catalytic effect of different exchangeable cations present on the surfaces of these coals on subsequent char reactivity in different atmospheres. This paper describes the results of such a study.

EXPERIMENTAL

Char Preparation. A Darco (Texas) lignite (28x48 mesh) was demineralized by boiling with 10% HCl and subsequently with a 50-50 mixture of 50% HF-10% HCl. The carboxyl content of the demineralized coal was 2.4 mmoles/g. Schafer's method was used to effect cation-exchange (5). Demineralized (Dem) lignite was contacted with 0.10 molar solutions of sodium acetate, potassium acetate, calcium acetate, magnesium acetate and ferric nitrate. Approximately 0.3 mmoles of cation per gram of coal were exchanged from the various solutions in 24 hr. Ten levels of exchangeable calcium ions in the range 0.10 to 2.14 mmoles/g of coal were introduced by contacting the Dem coal with calcium acetate solutions varying in concentration from 0.04 to 2.0 molar for 24 hr.

Raw, Dem and cation-exchanged samples were carbonized in N_2 in a fluidized bed. In each case, the sample was heated up to 800°C at a rate of 10°C/min. Soak time at 800°C was 2 hr.

Reactivity Measurements

Reactivities of various char samples were measured in air (1 atm, 390°C), CO_2 (1 atm, 760°C), steam (1 atm, 650°C), H_2 (1 atm, 790°C), 50% CO-50% H_2 mixture (total pressure 1 atm, 790°C), N_2-H_2O mixture (790°C), H_2-H_2O mixture (790°C), H_2-N_2-H_2O mixture (790°C) and CO-H_2-H_2O mixture (790°C). The partial pressure of water vapor in the last four mixtures (total pressure 1 atm) was 12.8 torr. This pressure was generated by bubbling the gas through deaerated distilled water thermostated at 15°C.

*Present Address: Standard Oil Co. (Indiana), Amoco Research Center, P. O. Box 400, Naperville, IL 60540

Reactivity measurements in 1 atm steam were carried out in a fluid bed reactor. Weight losses occurring during gasification in the other atmospheres studied were monitored using a DuPont 951 TGA system in conjunction with a 990 Thermal Analyzer. Details of the experimental procedures for reactivity measurements have been described elsewhere (6).

In the text, reactivity parameter, R, has been defined as:

$$R = \frac{1}{W_0} \cdot \frac{dW}{dt}$$

where W_0 is the initial char weight (daf) and dW/dt is the maximum rectilinear weight loss rate.

RESULTS AND DISCUSSION

Burn-off versus time plots for various char samples reacted in air are shown in Figure 1. The Dem char is significantly less reactive than the raw char. This has previously been attributed to the loss of catalytic inorganic matter upon demineralization (6). The following order of reactivities is observed for chars produced from raw, Dem and cation-exchanged samples:

$$Na > K > Ca > Raw > Fe > Mg > Dem$$

These results clearly show that the replacement of surface H^+ ions of carboxylic acid groups present on the surface of Dem lignite by metal cations increases the reactivity of the chars produced, but the extent of the increase is markedly dependent upon the nature of the cation. The higher reactivity of the char produced from the raw lignite compared to the iron and magnesium containing chars is thought to be due to the presence of catalytically active calcium ions in the raw lignite.

The following order of reactivities for various char samples was observed for the reaction in CO_2:

$$Na > K \sim Ca > Raw > Fe \gtrsim Dem > Mg$$

and in steam:

$$K > Ca > Na > Fe > Raw > Mg > Dem$$

Even though the $C\text{-}O_2$, $C\text{-}CO_2$ and $C\text{-}H_2O$ reactions all involve an intermediate oxygen transfer step followed by a gasification step, the order of reactivities of chars produced from different cation-exchanged samples is not the same in the three atmospheres. This shows the high specificity of different catalytic species.

For the various calcium containing chars, the reactivity parameter in air, CO_2 and steam increased linearly with increase in the amount of calcium present in the char. Furthermore, normalized reactivities of these chars in the three oxidizing atmospheres were essentially the same.

Burn-off plots for various char samples in H_2 are shown in Figure 2. The order of reactivities of various samples in H_2 is markedly different from that observed in the three oxidizing atmospheres. Below 45% burn-off, sodium is the most effective hydrogasification catalyst; whereas at higher burn-offs iron is a better catalyst. It is noteworthy that even though calcium and potassium are excellent oxidation catalysts, chars containing these species are much less reactive in H_2 than the raw char. In fact, for the various calcium-containing

samples reactivity in H_2 decreased monotonically with increase in calcium loading.

Two extreme cases of the effect of H_2 addition to steam on char reactivity are illustrated by the plots in Figures 3 and 4. At one extreme, for the raw char (Figure 3), which has calcium as the major inorganic impurity, gasification is more rapid in wet N_2 than in wet H_2. At the other extreme, the char produced from the iron exchanged sample has a higher reactivity in wet H_2 than in wet N_2 (Figure 4). It is known that in the elemental form iron is a good oxidation catalyst but in the oxide form it is a poor catalyst (7). In the present study, when the iron-containing char is reacted with wet H_2, the percentage of H_2 in the mixture is sufficient to keep iron in the reduced state.

In the CO-H_2 mixture, chars produced from raw and Na, K, Ca and Mg exchanged samples showed little or no weight loss. However, in the CO-H_2-H_2O mixture small but finite gasification rates were observed and the order of reactivity for various samples was:

$$Fe > Na > K > Ca > Raw > Mg$$

Results for the iron-containing char were unique (Figure 5). In the CO-H_2-H_2O mixture, the gasification rate is significantly lower than in N_2-H_2O or N_2-H_2-H_2O mixtures. Further, in the dry CO-H_2 mixture, after a slight initial weight loss, there is a rapid continuous increase in weight. This increase is attributed to the disproportionation of CO:

$$2\ CO \rightarrow CO_2 + C$$

For this reaction, iron is an excellent catalyst but is gradually deactivated due to the formation of cementite (8). In this study, the amount of H_2 in the CO-H_2 mixture is sufficient to keep iron in the catalytically active form, that is as elemental iron. Even though iron is an excellent catalyst for the C-H_2 reaction (7), it appears that in the presence of CO the weight increase due to disproportionation of CO offsets any weight loss due to hydrogasification.

ACKNOWLEDGEMENTS

This research was supported by DOE on Contract EX-76-C-01-2030. Professor W. Spackman, Jr. supplied the lignite used in this study. We appreciate the assistance of A. Linares-Solano on preliminary portions of this study.

REFERENCES

1. Jenkins, R. G., Nandi, S. P. and Walker, P. L., Jr., Fuel, 52, 288 (1973).

2. Hippo, E. and Walker, P. L., Jr., Fuel, 54, 245 (1975).

3. Linares-Solano, A., Mahajan, O. P. and Walker, P. L., Jr., "Reactivity of Heat Treated Coals in Steam " Fuel, in press.

4. Tomita, A., Mahajan, O. P. and Walker, P. L., Jr., Fuel, 56, 137 (1977).

5. Schafer, H. N. S., Fuel, 49, 197 (1970).

6. Mahajan, O. P. and Walker, P. L., Jr., in "Analytical Methods for Coal and Coal Products " (Ed. C. Karr, Jr.), Vol. 2, Academic Press, 1978, pp. 465-494.

7. Walker, P. L., Jr., Shelef, M. and Anderson, R. A. in "Chemistry and Physics of Carbon " (Ed. P. L. Walker, Jr.), Vol. 4, Marcel Dekker, New York, 1968, pp. 287-380.

8. Walker, P. L., Jr., Rakszawski, J. F. and Imperial, G. R., J. Phys. Chem., 63, 140 (1959).

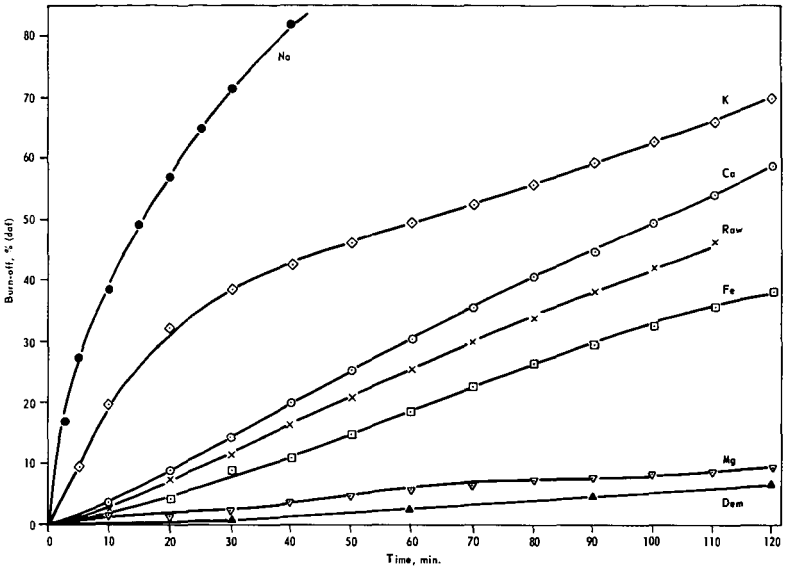

Figure 1. GASIFICATION OF LIGNITE CHARS IN AIR AT 390°C

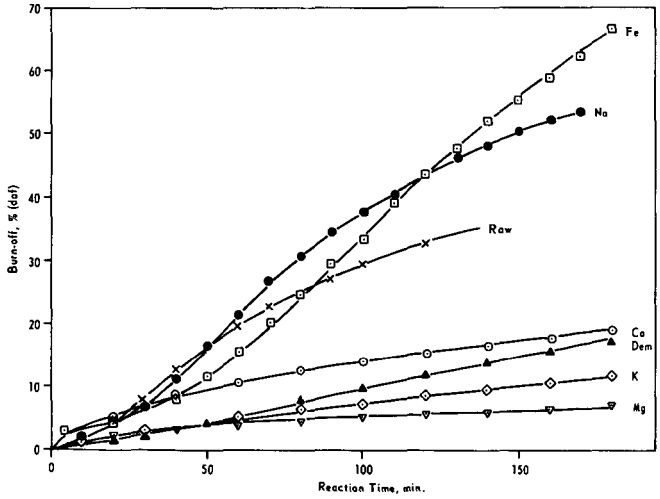

Figure 2. GASIFICATION OF LIGNITE CHARS IN 1 ATM H_2 AT 790°C

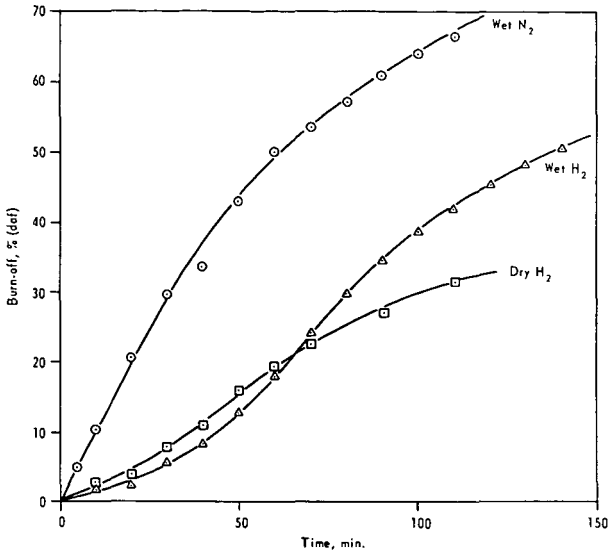

Figure 3. GASIFICATION AT 790°C OF CHAR PRODUCED FROM RAW LIGNITE IN VARIOUS ATMOSPHERES

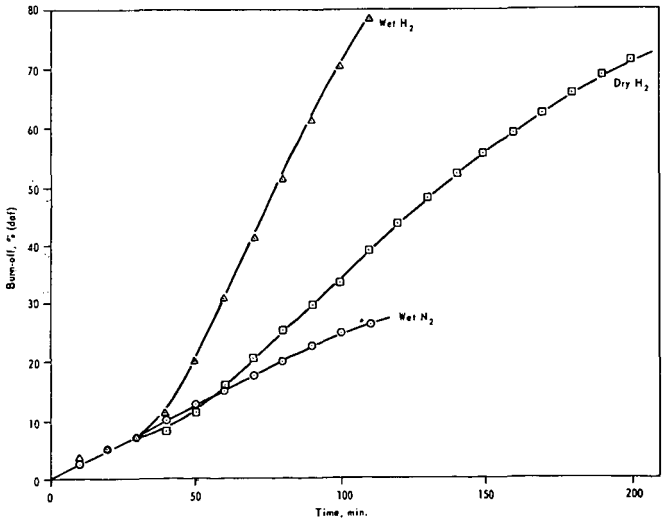

Figure 4. GASIFICATION AT 790°C OF IRON - CONTAINING CHAR IN VARIOUS ATMOSPHERES

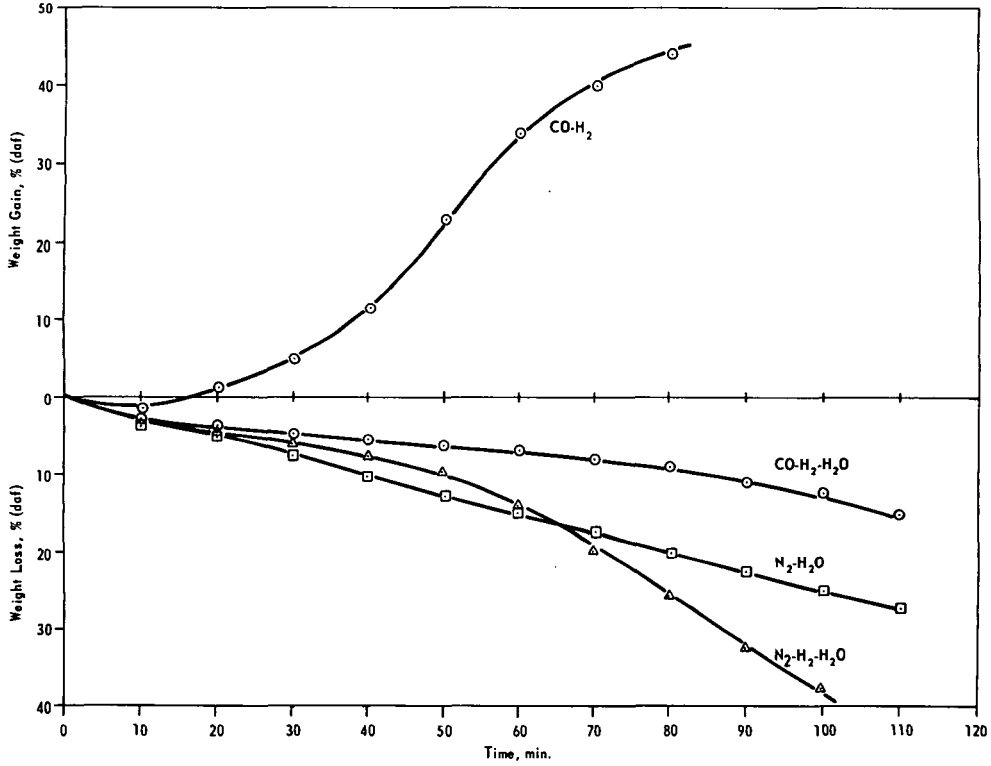

Figure 5. WEIGHT CHANGES FOR IRON-CONTAINING CHARS AT 790 °C IN THE PRESENCE OF VARIOUS ATMOSPHERES

CATALYTIC GASIFICATION OF LIGNITE CHARS

S.P. Nandi and J.L. Johnson

Institute of Gas Technology
3424 S. State St.
Chicago, Illinois 60616

INTRODUCTION

In a previous study (1), the kinetics of the gasification of chars derived from coals ranging from anthracite to lignite were determined in different gasification media. The relative reactivity factor decreased systematically with increasing carbon content in the parent coal. The overall decrease is caused both by decreasing surface areas and by decreasing specific surface reactivities of the chars. The correlations developed, however, do not generally apply to the lignite chars because of catalytic effects of exchangeable cations, particularly sodium and calcium, which are associated with the carboxyl groups of the lignites. Therefore, a systematic investigation was conducted to obtain detailed data describing the gasification characteristics of Montana and North Dakota lignite chars with particular emphasis given to determining the effect of sodium and calcium inherent or added by base exchange on the gasification rate. Calcium and sodium were chosen because these are the predominant exchangeable cations present in Montana and North Dakota lignites.

APPARATUS AND EXPERIMENTAL PROCEDURE

A high-pressure thermobalance was used in this work to obtain reaction rates. The main feature of this apparatus is that the weight of a small fixed-bed sample of char (approximately 0.5 gram) contained in a wire mesh basket can be continuously measured as it undergoes gasification in a desired environment at constant temperature and pressure. In all of the tests conducted, chars in -20+40 USS sieve size particles were used, and gas flow rates in the reactor were maintained at sufficiently high values to result in negligible gas conversion. The weight loss versus time characteristics obtained during individual tests were used to calculate the base carbon conversion fraction (1).

The proximate and ultimate analyses of the lignite samples are shown in Table 1. The acid-washed lignites were prepared from the original lignites by treatment with 1N HCl at room temperature followed by washing with distilled water until the effluents were chloride free. The wet samples were dried at 60°C under vacuum. The acid-washed lignites were treated, in turn, with solutions of sodium or calcium acetate, and a number of lignite samples of varying concentrations of base exchanged sodium and calcium were prepared. The nomenclature of the original and treated lignites, together with the concentration of sodium and calcium, is given in Table 2. Chars were prepared from samples by devolatilization in nitrogen (1 atmosphere) for 30 minutes at temperatures from 1400° to 1700°F. For these samples, devolatilization was essentially complete at the lowest temperature used, and the concentration of sodium and/or calcium for chars from the same starting lignite was assumed to be the same at different char preparation temperatures.

Gasification of the chars was conducted at the char preparation temperatures with hydrogen and equimolar steam-hydrogen mixtures at pressures ranging from 14.6 to 69.0 atmospheres. With one sample (G), gasification was conducted in synthesis gas mixtures. The compositions of the synthesis gas mixtures are shown in Table 3.

Table 1. ANALYSES OF LIGNITES

Sample	Proximate Analysis			Ultimate Analysis					
	VM	FC	Ash	C	H	O	N	S	Ash
	wt % dry			wt % dry					
Montana, Raw	43.6	51.3	5.1	65.13	4.13	24.20	0.89	0.57	5.08
Montana, Acid Washed	46.9	52.1	1.0	68.60	4.42	24.57	0.90	0.58	1.00
North Dakota, Raw	43.7	49.6	6.7	62.90	4.27	24.09	0.97	1.10	6.67
North Dakota, Acid Washed	45.8	52.5	1.7	67.70	4.33	24.38	1.00	0.90	1.69

Table 2. NOMENCLATURE OF THE SAMPLES AND THEIR SODIUM AND CALCIUM CONTENT

No.	Sample	Name	Concentration, g-atoms/g-atom base carbon		
			Na	Ca	Na + Ca
1.	Montana, Acid Washed	A	0.00000	0.00000	0.00000
2.	Montana, Ca-Ex. 1	B	0.00000	0.00139	0.00139
3.	Montana, Ca-Ex. 2	C	0.00000	0.00972	0.00972
4.	Montana, Raw	D	0.00164	0.01364	0.01528
5.	Montana, Na+Ca-Ex	E	0.01098	0.00505	0.01603
6.	Montana, Na-Ex. 1	F	0.00274	0.00000	0.00274
7.	Montana, Na-Ex. 2	G	0.01955	0.00000	0.01955
8.	North Dakota, Raw	N	0.00329	0.00758	0.01087
9.	North Dakota, Acid Washed	O	0.00000	0.00000	0.00000
10.	North Dakota, Ca-Ex	P	0.00000	0.01326	0.01326

Table 3. COMPOSITION OF SYNTHESIS GAS MIXTURES

	H_2	H_2O	CO	CO_2	CH_4
	vol %				
Syn-Gas 1	47.5	40.4	6.0	3.6	2.5
Syn-Gas 2	43.6	35.3	11.8	8.2	1.1
Syn-Gas 3	36.8	29.3	19.3	11.3	3.3

RESULTS AND DISCUSSION

Gasification in Hydrogen

Initial gasification tests in hydrogen were conducted with Montana and North Dakota chars obtained from acid-treated lignites to provide a basis for determining gasification kinetics in the absence of exchangeable cations. Typical results are shown in Figures 1 and 2. The results show that, at a given temperature, gasification rates increased significantly with increasing hydrogen pressure. Similarly, at a constant hydrogen pressure, gasification rates increase significantly with increasing temperature. For Montana char, a carbon conversion of approximately 0.09, which tends to be independent of temperature and pressure, occurred during the heat-up period of char (which takes about 1 to 2 minutes after lowering the sample to the reaction zone). It was hypothesized that Montana chars contain two types of carbon - Type I, which gasifies very rapidly during the heat-up period, and Type II, which is subsequently gasified. For North Dakota chars, only Type II carbon was indicated.

In previous studies (2) with bituminous coal chars, gasification kinetics in hydrogen was described by the expression —

$$\frac{dX}{dt} = f_L K_H (1-X) \qquad 1)$$

where —

X = base carbon fraction

t = time, min

K_H = rate constant for reference char ($f_L = 1$), min^{-1}.

The rate constant was determined by the equation —

$$K_H = \frac{P^2_{H_2} \exp (2.674 - 24{,}609/T)}{1 + P_{H_2} \exp (-10.452 + 19.976/T)} \qquad 2)$$

where —

f_L = relative reactivity factor

T = temperature, °R

P_{H_2} = hydrogen partial pressure, atm.

Figure 3 shows the -ln(1-X) versus reaction time plots for the experimental results of gasification in hydrogen for Montana lignite chars. Also included in the figure is the calculated base carbon conversion fraction for the reference bituminous coal char (char from preoxidized Pittsburg No. 8 seam coal). The experimental base carbon conversion data for Montana lignite are nonlinear when plotted according to Equation 1. The curve for the char from Raw Montana starts with a high initial slope; however, the value of the slope decreases with the increase of X and, at high value of X, becomes lower than that for the reference bituminous char. Upon removal of exchangeable cations, the reactivity of char decreases and the extent of nonlinearity is diminished but not entirely removed.

To take into account the characteristics of lignite char gasification mentioned above, it has been assumed that there are two transient reactions in addition to the low-rate gasification reactions that determine the rate of lignite char gasification. The first transient reaction is assumed to be catalyzed by some structural component present in lignite char, and the second transient reaction is assumed to be catalyzed by the exchangeable cations present in lignite. It is also assumed that the low-rate gasification of lignite char is kinetically similar to the low-rate gasification occurring in bituminous coal char.

The following reaction model was proposed: The Montana lignite char is composed of two types of carbon. In the presence of hydrogen, a fraction of carbon (Type 1) is gasified very rapidly to methane during the heat-up period (1 to 2 minutes in thermobalance tests). The remaining carbon (Type 2) gasifies by three possible paths, as indicated below:

$$C\ (\text{Type 2}) + H_2 \xrightarrow[n^*]{K_i^*} CH_4\ (\text{Reaction I}) \qquad 3a)$$

$$C\ (\text{Type 2}) + H_2 \xrightarrow[n^{**}]{K_i^{**}} CH_4\ (\text{Reaction II}) \qquad 3b)$$

$$C\ (\text{Type 2}) + H_2 \xrightarrow{f_L K_H} CH_4\ (\text{Reaction III}) \qquad 3c)$$

Reaction III is assumed to be similar to the reaction path followed by bituminous coal char (low-rate gasification). The parameters f_L and K_H have been defined (2). Reaction I corresponds to a path in which some entity, n*, catalyzes gasification. The entity n* is assumed to be a structural component present in char. It is also assumed that n* deactivates by a first-order process. For Reaction II, n** is a metal, catalyst-containing complex that catalyzes this reaction. Similar to Reaction I, it was assumed that n** also deactivates by a first-order process.

With the above assumptions, the following rate expression results —

$$-\ln(1-X) = -\ln(1-X^*) + \frac{K_i^* C_o^{n^*}}{K_o^*}(1-e^{-K_o^* t}) + \frac{K_i^{**} C_o^{n^{**}}}{K_o^{**}}(1-e^{-K_o^{**} t}) + f_L K_H t \qquad 4)$$

The different parameters of Equation 4 were evaluated from experimental data. For chars from both lignites —

$$K_o^* = K_o^{**} = 5.74 \exp(-9770/T) \qquad 5)$$

Particular evaluations for chars from Montana lignite are the following:

$$f_L = 0.70$$

$$X^* = 0.086$$

$$\frac{K_i^* C_o^{n^*}}{K_o^*} = 0.026\ P_{H_2}^{1/2}$$

$$K_i^{**} C_{n^{**}} = (380 C_{Na} + 32 C_{Ca})\ f_L\ K_H \qquad 6)$$

where C_{Na} and C_{Ca} are concentrations of sodium and calcium, g-atom/g-atom base carbon.

Equation 4 was used with the evaluation given above to calculate the base carbon conversion for the chars from Raw Montana lignite. In Figure 4, the solid line represents the calculated values of X. The experimental points shown follow the line closely except for the first 5 minutes of reaction time. A similar match was obtained for the other char samples.

Particular evaluations for chars from North Dakota lignite are the following:

$$f_L = 0.85$$

$$X^* = 0.0$$

$$\frac{K^* C^o_{i\,n^*}}{K^*_o} = 0.045\, P_{H_2}^{1/2}$$

$$K^{**} C^o_{i\,n^{**}} = (500 C_{Na} + 75 C_{Ca})\, f_L\, K_H \qquad 7)$$

The evaluation of the term $K^{**} C^o_{i\,n^{**}}$, in terms of catalyst concentration show that, for both lignites, sodium was a better catalyst than calcium for hydrogasification. This observation can also be verified by choosing the time for 50% ($T_{0.5}$) carbon conversion as a rate parameter. The time to reach a certain fraction of carbon conversion is a measure of reaction rate even for a reaction which is not first-order (3). The $T_{0.5}$ values are presented in Table 4 for different chars obtained from Montana lignite. The $1/T_{0.5}$ values of the chars containing only sodium or only calcium are shown in Figure 5, plotted against the concentration of Na or Ca. The values for the acid-washed lignite chars are also shown. It is clear that calcium is a poor catalyst for hydrogasification.

Table 4. TIME FOR 50% BASE CARBON CONVERSION OF MONTANA CHARS

Sample	Reaction Temperature, °F	Hydrogen Pressure, atm	$T_{0.5}$, min (time for X=0.5)	$\frac{1}{T_{0.5}}$, min^{-1}
A	1600	35	100.0	0.0100
A	1700	35	39.0	0.0256
A	1600	69	44.0	0.0227
A	1700	69	18.5	0.0540
B	1600	35	105.0	0.0095
B	1700	35	34.0	0.0294
C	1600	35	100.0	0.0100
C	1700	35	31.0	0.0322
D	1600	35	78.0	0.0128
D	1700	35	26.5	0.0377
E	1600	35	48.5	0.0206
E	1700	35	19.0	0.0526
E	1600	69	11.8	0.0847
E	1700	69	4.5	0.2222
F	1600	35	68.0	0.0147
F	1700	35	23.5	0.0425
G	1600	35	20.5	0.0488
G	1700	35	9.0	0.1111

Gasification in Equimolar Steam-Hydrogen Mixtures:

Gasification in equimolar steam-hydrogen mixtures was conducted with different char samples at temperatures of 1500° to 1700°F and at pressures of 14.6 to 69.0 atmospheres. The effect of total pressure on gasification for char, obtained from acid-washed North Dakota lignite is shown in Figure 6. The rate of gasification increased with the increase of total pressure. These results were anticipated because at higher total pressure, the partial pressure of hydrogen will be higher; that alone could enhance the rate of gasification, even if the rate was independent of steam partial pressure. In contrast, it was observed that, for samples containing Na or Ca, the gasification rate in this medium was independent of total pressure. Typical results indicating this behavior are presented in Figure 7. In this context, Vadovic and Eakman (4) have shown that for steam gasification of chars catalyzed by potassium, the rate was independent of steam partial pressure. The results of the current investigation indicate that, for chars containing Na or Ca as catalyst, the gasification rate is controlled by the steam-carbon reaction, even though the gasification medium contains 50% hydrogen. For all of the char samples, the rate of gasification in equimolar steam-hydrogen mixtures increased with temperature. Typical gasification data for chars containing different amounts of catalyst are shown in Figure 8.

It has been shown (2) that, with bituminous coal chars, gasification in steam-hydrogen mixtures could be correlated by the expression —

$$\frac{dX}{dt} = f_L K_T (1-X)^{2/3} \exp(-\alpha X^2) \qquad 8)$$

Integrating Equation 8, we obtain —

$$M(X) = \int_0^X \frac{\exp(\alpha X^2)}{(1-X)^{2/3}} = f_L K_T + I \qquad 9)$$

where —

K_T = overall rate constant

f_L = relative reactivity factor

α = kinetic parameter dependent on gas composition

I = integration constant.

For bituminous coal chars, which were devolatilized at temperatures of 1400°F or higher, I = 0.0, and α, for equimolar steam-hydrogen mixtures, is equal to 1.67. The char gasification data of this study was analyzed by Equation 9 assuming α to be equal to 1.67. Typical plots of M(X) versus time for three char samples are shown in Figure 9. Linear plots of up to a value of X=0.86 were obtained, but all the lines do not pass through the origin. The acid-washed lignite chars tend to have an intercept of about 0.1. The slope and intercept values of all the chars tested are shown in Table 5. In Figure 10, the values of the overall rate constant ($f_L K_T$) for steam-hydrogen gasification of Montana chars are plotted against the total concentration of sodium and/or calcium present in the char. All of the experimental points, whether the char contained only sodium, only calcium, or their mixture, tended to fall on the same line at a particular temperature, indicating that, in steam-hydrogen mixtures, calcium is as effective a catalyst as sodium. For Montana chars, the increase of rate with the increase of catalyst concentration and temperature can be correlated by the following experimental equation:

$$\text{Overall rate} = f_L K_T = [C_{(Na+Ca)} + 0.0032]\exp(19.80 - 38000/T) \qquad 10)$$

Table 5. KINETIC PARAMETERS FOR GASIFICATION OF CHARS FROM MONTANA AND NORTH DAKOTA LIGNITES IN EQUIMOLAR STEAM-HYDROGEN MIXTURES

Char Source	Temperature, °F	$f_L K_T$ (Slope)	I (Intercept)
A	1500	0.0030	0.10
A	1600	0.0082	0.10
A	1700	0.0262	0.08
B	1500	0.0050	0.10
B	1600	0.0240	0.08
B	1700	0.0473	0.10
C	1600	0.0546	0.05
C	1700	0.1175	0.00
D	1500	0.0235	0.06
D	1600	0.0796	0.00
D	1700	0.1640	0.00
F	1600	0.0340	0.05
F	1700	0.1000	0.00
G	1500	0.0332	0.08
G	1600	0.0954	0.00
G	1700	0.1892	0.00
O	1500	0.0046	0.05
O	1600	0.0136	0.09
O	1700	0.0249	0.08
N	1500	0.0410	0.00
N	1600	0.0972	0.00
N	1700	0.1680	0.00
P	1500	0.0502	0.00
P	1600	0.1050	0.00
P	1700	0.2205	0.00

For North Dakota chars, the following correlations satisfy the experimental results:

$$\text{Overall rate} = f_L K_T = [C_{(Ca+Na)} + 0.0015]\exp(16.58 - 30000/T) \qquad 11)$$

The gasification characteristics of chars from two lignites having similar elemental compositions are qualitatively similar, but, the numerical magnitude of the rate parameters differ. That is, enhancement of rate by a catalyst is dependent upon the nature of the char on which the catalyst is distributed.

Gasification in Synthesis Gas Mixtures

Gasification of one sample of char from Montana lignite was conducted in synthesis gas (syn-gas) mixtures. Tests were done with Syn-Gas 2 at 35 and 69 atmospheres at a temperature of 1700°F, and it was noted that the rate of base carbon conversion was the same at both pressures. The effect of pressure on rate of gasification in synthesis gas mixtures seems to be the same as was observed for gasifi-

cation in steam-hydrogen mixtures. The results of gasification with different syn-gas mixtures are shown in Figure 11. The gasification data in equimolar steam-hydrogen mixtures are also shown in this figure. The (P_{H_2}/P_{H_2O}) ratio for the syn-gas mixtures are 1.18, 1.23, and 1.25 for the three mixtures shown in Table 3. The (P_{CO}/P_{H_2O}) ratios are 0.15, 0.33, and 0.66. Therefore, the main compositional variable between the three synthesis gas mixtures is the CO/H_2O ratio. The effect of CO_2 and CH_4 in the mixture was considered to be minor. It is seen from Figure 11 that at the same temperature and pressure, the rate of carbon conversion decreases with the increase of the CO/H_2O ratio. The overall rate constants ($f_L K_T$) for the gasification in syn-gas was calculated with Equation 9. The values are 0.100, 0.076, and 0.039 respectively, for the three mixtures. It is seen that, for char from Sample G the rate of gasification in equimolar steam-hydrogen mixtures was approximately five times higher compared with that for Syn-Gas 3.

CONCLUSIONS

For gasification of lignite chars in hydrogen, sodium was more efficient as a catalyst than calcium. The gasification rate of lignite chars containing sodium or calcium remains essentially constant with the increase of total pressure in steam-hydrogen and synthesis gas mixtures. Both calcium and sodium enhance the rate of gasification of lignite chars in steam-hydrogen mixtures, and the effect is proportional to the concentration (g-atom/g-atom carbon) of sodium and/or calcium present. The catalytic effect of sodium or calcium depends on the nature of char on which the catalyst is dispersed; that is, the same concentration of sodium does not produce the same quantitative effect on rate for chars obtained from lignites having similar elemental composition. The catalysts tend to selectively enhance the rate of the steam-carbon reaction, preferring the carbon-hydrogen reaction when gasification is conducted in steam-hydrogen mixtures.

LITERATURE CITED

1. Johnson, J.L., "Relation Between the Gasification Reactivity of Coal Chars and the Physical and Chemical Properties of Coals," ACS Div. Fuel Chem. Prepr. 20, No. 4, 85 (1975).
2. Johnson, J.L., "Kinetics of Bituminous Coal Char Gasification With Gases Containing Steam and Hydrogen," Advances in Chemistry Series 131, 145 (1974).
3. Mahajan, Om.P.,Yarzab, R. and Walker, P.L., Jr., "Unification of Coal Char Gasification Mechanism," Fuel 57, 643 (1978).
4. Vadovic, C.J. and Eakman, J.M., "Kinetics of Potassium Catalysted Gasification," ACS Div. Fuel Chem. Prepr. 23, No. 8, 89 (1978).

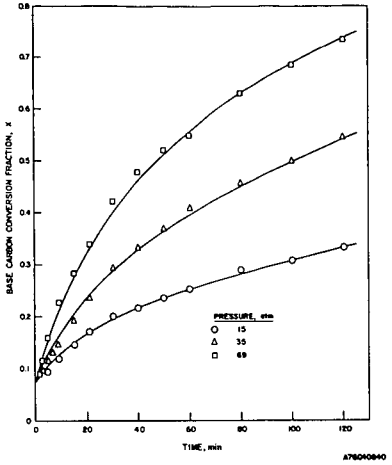

Figure 1. CONVERSION OF ACID-TREATED MONTANA LIGNITE CHAR IN HYDROGEN AT 1600°F

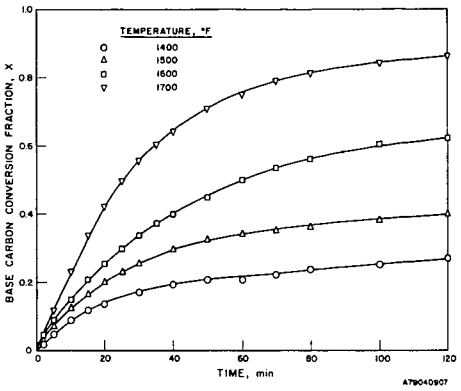

Figure 2. GASIFICATION OF ACID-WASHED NORTH DAKOTA CHARS IN HYDROGEN AT 35 atm

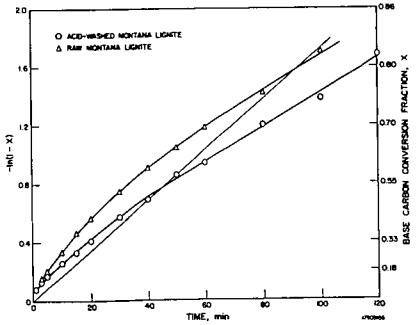

Figure 3. GASIFICATION OF RAW AND ACID-WASHED MONTANA LIGNITE CHARS IN HYDROGEN AT 1700°F AND 35 atm

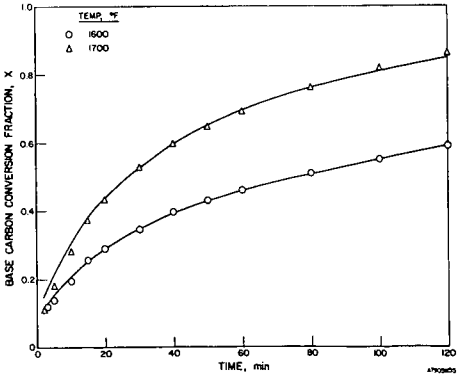

Figure 4. GASIFICATION OF RAW MONTANA CHARS IN HYDROGEN AT 35 atm

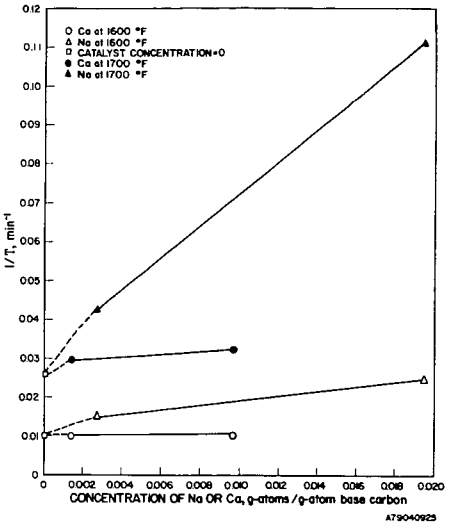

Figure 5. EFFECT OF CATALYST CONCENTRATION ON THE RECIPROCAL TIME FOR 50% BASE CARBON CONVERSION

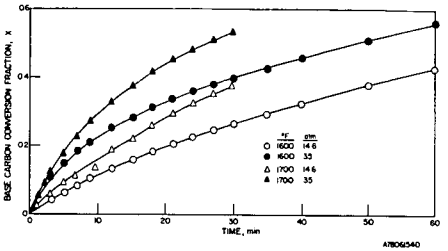

Figure 6. GASIFICATION OF ACID-WASHED NORTH DAKOTA CHARS IN STEAM-HYDROGEN MIXTURES (H_2O/H_2 = 1)

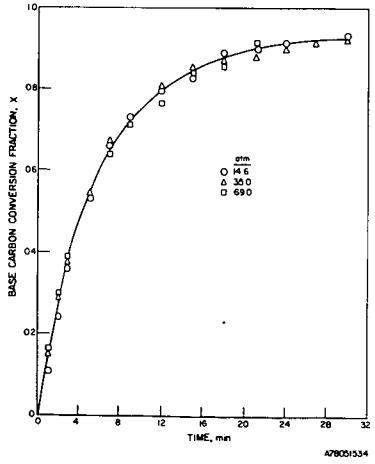

Figure 7. EFFECT OF PRESSURE ON THE GASIFICATION OF NORTH DAKOTA RAW CHAR IN STEAM-HYDROGEN MIXTURES (H_2O/H_2=1) AT 1700°F

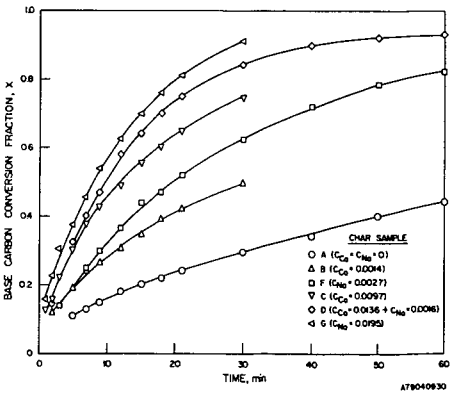

Figure 8. GASIFICATION OF MONTANA CHARS IN EQUIMOLAR STEAM-HYDROGEN MIXTURES AT 1600°F AND 35 atm

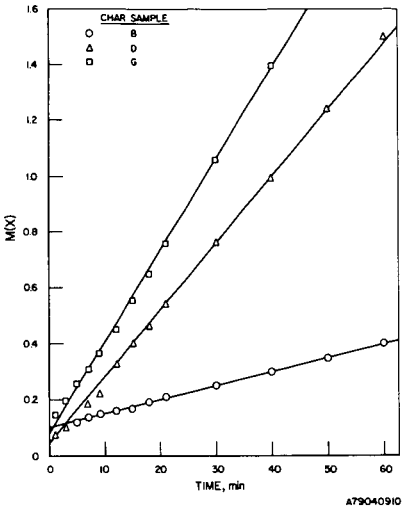

Figure 9. BASE CARBON CONVERSION FUNCTION VS. TIME PLOTS FOR THE GASIFICATION OF MONTANA LIGNITE CHARS IN EQUIMOLAR STEAM-HYDROGEN MIXTURES AT 1500°F AND 35 atm

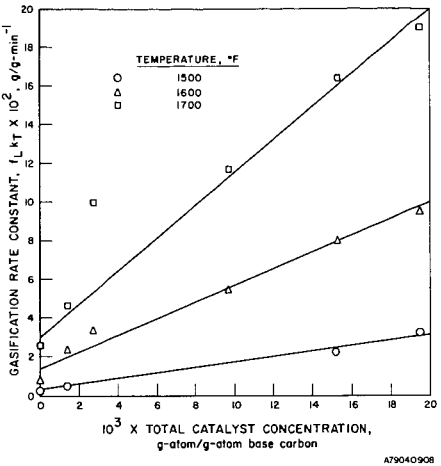

Figure 10. EFFECT OF CATALYST CONCENTRATION ON THE OVERALL RATE OF GASIFICATION OF MONTANA LIGNITE CHARS IN EQUIMOLAR STEAM-HYDROGEN MIXTURES AT A TOTAL PRESSURE OF 35 atm

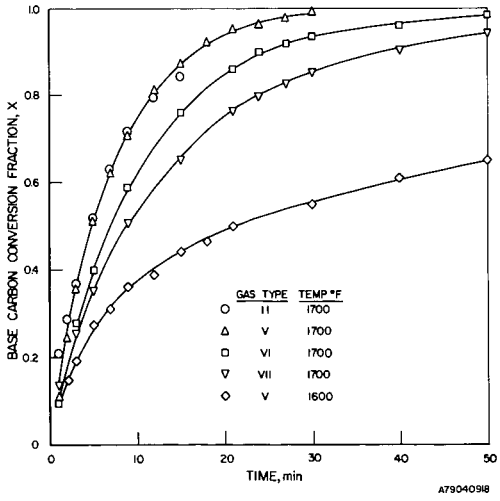

Figure 11. GASIFICATION OF CHARS FROM SAMPLE G IN SYNTHESIS GAS MIXTURES AT 35 atm

CHEMISTRY OF GASIFICATION AND ASH AGGLOMERATION IN THE U-GAS^{R} PROCESS.

J. G. Patel, D. M. Mason, 3424 South State Street, Chicago, IL 60616

A single-stage, fluidized-bed, ash-agglomerating process for generation of industrial fuel gas or synthesis gas from coal has been tested in a pilot plant with coke, char, and coal as feed. Pilot plant and laboratory data on gasification reactivities have been obtained and incorporated into a mathematical model. The chemistry of agglomeration of ash was investigated by methods including optical and electron microscopy, chemical analyses, and fusibility tests. Agglomeration of ash into rounded beads occurred with relative ease in runs on coke; the agglutinating agent is an iron-rich, relatively low-melting silicate in which other ash is embedded. Agglomeration of ash from coal was more difficult, because most of the iron was present in the form of sulfide and thus unavailable for reaction with aluminosilicates (clay minerals). The gas composition in the reactor bed is thermodynamically favorable for oxidation of the ferrous sulfide at regions near the oxygen inlet only. Oxidation of the ferrous sulfide and agglomeration of ash from coal were achieved by changing the mode of oxygen feed to the reactor.

REACTIVITY OF TRI-GAS CHAR IN A FLUIDIZED-BED REACTOR

Mario A. Colaluca, Kanwal Mahajan, Mark A. Paisley

Bituminous Coal Research, Inc.
350 Hochberg Road, Monroeville, Pennsylvania 15146

INTRODUCTION

The evolution and the development of the BCR TRI-GAS fluidized-bed gasification process to produce low- to medium-Btu fuel gas has been described in two earlier papers.[1,2] TRI-GAS is a multiple fluidized-bed coal gasification process. The overall objective of TRI-GAS is the gasification of a range of coals, with the only product being a clean, low-Btu fuel gas. No liquids, tar, or char are produced as a waste or by-product. The process consists of three fluidized-bed reactors connected in series. Each reactor has its own specific function. Stage 2 is the main gasification stage. In this stage, devolatilized coal (char) and the volatile products from Stage 1 are gasified with air and steam, producing a low-Btu (about 150 Btu/cu ft) fuel gas.

The objective of the current study is to establish a model for the overall gasification reaction in a fluidized bed and to use this model to predict conversion in the TRI-GAS Stage 2 reactor during PEDU tests. The model assumes that the overall reaction rate is determined by the separate rates of two processes in series; first, mass transfer, where steam must be transported out of the bubble to the particulate phase, and second, the chemical reaction. The chemical reaction process has been isolated from mass-transfer effects and studied independently in the thermogravimetric analysis (TGA) unit where a chemical reaction rate is established, describing the resistance of the chemical process. Similarly, the tests in the bench-scale fluidized-bed reactor establish a parameter characterizing the mass transfer process from the bubble to the particulate phase.

APPARATUS AND PROCEDURE

Char Preparation

Char (+100 mesh) from the Rosebud seam coal pretreated during a typical PEDU test was used for reactivity studies in the TGA apparatus and the bench-scale fluidized-bed batch reactor. This char was produced by pretreating the Rosebud seam coal in a fluidized bed at 900 F to remove volatile matter and tars from the coal prior to feeding to the gasification reactor.

TGA Reactivity

An American Instrument Company basic thermogravimetric analysis unit was used for the reactivity measurements. About 100 mg of char contained in a ceramic pan was heated in nitrogen to the chosen reaction temperature. Since some devolatilization occurred during this process, heating continued until the char weight became constant. The nitrogen was then bubbled through water held at a specified temperature and this reactant passed over the char. Char weight loss was recorded continuously as a function of time.

The measure of reactivity chosen in this study was the same as Jenkins' "reactivity parameter".[3] The definition is (symbols defined in Appendix A):

$$R_5 = \frac{1}{W_o} \frac{dW}{dt}$$

The maximum rate of weight loss ($\frac{dW}{dt}$) was determined experimentally from the slope of the weight loss data recorded on an X-Y plotter. The maximum rate could be defined without difficulty since, in all cases, the initial rate was constant.

The reactivity parameter was assumed to depend on reacting gas concentration, C_p, in the following manner:

$$R_5 = k \quad C_p^n \tag{1}$$

where

$$k = \alpha \exp - \frac{E}{RT}$$

Taking the natural logarithm of both sides of Equation (1) results in

$$\ln R_5 = \ln k + n \ln C_p \tag{2}$$

A multiple linear regression analysis was performed using reaction rate (R_5) data taken at constant temperature for various values of C_p, resulting in values of n. The values of n, taken for several temperatures, were then averaged.

With n thus defined, Equation (1) can be used to determine the apparent activation energy and frequency factor for each reaction. Solving for k in Equation (1) results in

$$k = \frac{R_5}{C_p^n} \tag{3}$$

The right-hand side of this expression can be calculated from the data, the previously determined values of n, and the experimental conditions. Again, taking the logarithm of both sides results in

$$\ln k = \ln \frac{R_5}{C_p^n} = \ln \alpha - \frac{E}{RT} \tag{4}$$

A multiple regression analysis was performed using data at several temperatures resulting in the "apparent" activation energy E and the frequency factor α for each reaction. These results are reported in Table 1.

TABLE 1. TGA REACTIVITIES AND KINETIC PARAMETERS OF CHAR USED IN LABORATORY STUDIES

Test No.	Sample Temp, °K	Volatile Matter, mg	Steam Concentration, moles/cu cm	Reactivity, $(hr)^{-1}$
1	1193	12.8	0.89×10^{-6}	2.21
2	1193	13.3	1.35×10^{-6}	3.11
3	1193	13.5	2.01×10^{-6}	3.76
4	1136	11.5	0.93×10^{-6}	1.67
5	1136	12.0	1.42×10^{-6}	2.12
6	1136	11.5	2.11×10^{-6}	2.67

$$R_5 = C_p^n \quad \alpha \exp^{-E/\bar{R}T}$$

$$n = 0.61$$

$$\alpha = 1.94 \times 10^7$$

$$E = 17{,}662 \text{ cals}$$

Fluidized-bed Reactor

A schematic of the bench-scale fluidized-bed pressurized batch reactor system is shown in Figure 1. This system can be used for reactivity analysis with steam, carbon dioxide, and air. The reactor is made of 5.08 cm diameter by 91 cm long Incoloy 800 pipe. The reactor furnace consists of two 1450 watt, 61 cm long, furnace half-sections. The steam is generated by bubbling the inert gas through a 10.16 cm diameter by 51 cm long 316SS water-filled vessel heated by 2KW immersion heater. This steam generator is capable of producing saturated steam at 150 psi pressure. The reactor is followed by a water-cooled vessel where condensibles can be collected. The precise metering of the reacting gases is accomplished through Brooks Instrument Model 1110 rotameters. Foxboro pressure and DP cell transmitters are used for pressure control in the system and differential pressure measurements in the bed. For efficient distribution of the reacting gases in the reactor, the grid system consists of a 5-cm fixed bed of Steatite packing, packed between two screens. The system is also equipped with necessary auxiliary equipment for indicating actual pressures and temperatures in the reactor and the boiler. The system can be used to generate the reactivity data at 2200 F temperature and 150 psi pressure.

A 200-gm sample of the char was heated to the chosen reaction temperature and pressure with nitrogen flowing through the bed. Then the water-vapor reactant was generated by bubbling the nitrogen through hot water at a specified temperature and passed through the reactor. After a specified period of time, the reaction was quenched when the bed was purged with nitrogen. Conversion was determined by weighing the sample after cooling.

In a fluidized-bed reactor, the experimental value of the percent unreacted char is given by:

$$Y_{exp} = \frac{W}{W_o} \times 100$$

THEORETICAL MODEL

The model assumes that the overall reaction rate is determined by the separate rates of two processes in series; first, mass transfer, where steam must be transported out of the bubble to the particulate phase, and second, the chemical reaction. The chemical reaction process has been isolated from mass-transfer effects and studied independently in the thermogravimetric analysis (TGA) unit where a chemical reaction rate constant describing the resistance of the chemical process was established.

The following development is essentially that presented by Orcutt.[4] Only the detailed form of the reactant conversion term (R_c) differs. The form used in this study was developed empirically from differential reactor (TGA) data. The fluid bed is assumed to be divided into two distinct phases called the bubble and particulate phase. The reactant flow above that required to just fluidize the bed forms the bubble phase. No solids exist in this phase so no chemical reactions can occur. It is assumed that the bubble size is uniform. The particulate phase consists of the remainder of the flow and the solid char. The char-steam chemical reaction occurs in the particulate phase. Furthermore, the turbulent action in the bed allows the assumption that the steam concentration and temperature are constant throughout the particulate phase.

A material balance on a single rising bubble gives:

$$U_B V \frac{dC_B}{dy} = Q\,(C_P - C_B) \qquad (1)$$

Since C_P is assumed to be a constant, Equation (1) can be integrated directly to obtain:

$$\int_{C_O}^{C_B} \frac{dC_B}{C_P - C_B} = \frac{Q}{U_B V} \int_0^y dy$$

$$C_B = C_P + (C_0 - C_P) \exp^{-X(y)} \tag{2}$$

where $$X(y) = \frac{Qy}{U_B V}$$

The particulate phase material balance is:

$$R_1 + R_2 = R_3 + R_4 + R_5 \tag{3}$$

The amount of reactant transferred from the bubble, R_1, is determined by integrating the flow from the individual bubbles to the particulate phase over the entire reactor:

$$R_1 = A_T\, NQ \int_0^L C_B\, dy$$

Using Equation (2) for C_B results in:

$$R_1 = A_T\, NQ \left[C_P L - (C_0 - C_P) \frac{U_B V}{Q} \exp^{-X(L)} + (C_0 - C_P) \frac{U_B V}{Q}\right] \tag{4}$$

The amount of reactant fed directly to the particulate phase is:

$$R_2 = A_T\ U_{mf}\ C_0 \tag{5}$$

and leaving the particulate phase is:

$$R_4 = A_T\ U_{mf}\ C_P \tag{6}$$

The amount of reactant transported from the particulate to the bubble phase is given by:

$$R_3 = A_T\, NQ\, L\, C_P \tag{7}$$

Finally, the reactant consumed by the gasification reaction in the particulate phase is given by:

$$R_5 = A_T\, L_{mf} \left(\frac{1}{V_{TMF}} \frac{dN_R}{dt}\right) \tag{8}$$

The TGA data are used to evaluate the right-hand side of Equation (8). The TGA reaction rate is given by:

$$\frac{1}{W_o}\ \frac{dW}{dt} = -k\ C_P^n\ \frac{W}{W_o} \tag{9}$$

But,

$$dW = M_C\ dN_C$$

Thus,

$$\frac{dN_C}{dt} = -\frac{W_o}{M_C}\ k\ C_P^n\ Y$$

For the reaction:

$$C + H_2O \longrightarrow CO + H_2$$

$$\frac{dN_C}{dt} = \frac{dN_R}{dt}$$

so that,

$$\frac{1}{V_{TMF}}\ \frac{dN_R}{dt} = -\frac{W_o}{M_C\ V_{TMF}}\ k\ C_P^n\ Y \tag{10}$$

Substituting this expression into Equation (8) gives:

$$R_5 = \frac{A_T\ L_{mf}}{V_{TMF}}\ \left(\frac{W_o}{M_C}\right) k\ C_P^n\ Y \tag{11}$$

Substituting Equations (4), (5), (6), (7), and (11) into Equation (3) gives:

$$(VNU_B)\ (C_O - C_P)\ (1 - \exp^{-X(L)}) + U_{mf}\ (C_O - C_P) = \frac{1}{A_T}\ \frac{W_o}{M_C}\ k\ C_P^n\ Y$$

From Reference 6

$$VNU_B = U_o - U_{mf}$$

and defining:

$$\beta = 1 - \frac{U_{mf}}{U_o}$$

$$\xi_P = \frac{C_P}{C_O}$$

and

$$\lambda = \frac{W_o}{M_C} \frac{k\, C_o^{n-1}}{A_T\, U_o}$$

the nondimensional form for the particulate phase balance becomes,

$$(1 - \xi_p)\ [\beta\ (1 - \exp^{-X(L)}) + (1 - \beta)] = \lambda\ Y\ \xi_p^n \ . \quad (12)$$

In nondimensional form, Equation (9), describing the char conversion, becomes:

$$\frac{dY}{d\tau} = - \gamma\ \xi_p^n\ Y \quad (13)$$

where

$$\tau = \frac{t}{t_R}$$

$$\gamma = k\ C_O^n\ t_R$$

To compare this model with data from the batch laboratory tests, Equation (13) is integrated numerically to determine char weight for various run times. For each integration step, Equation (12) is solved for ξ_p.

RESULTS AND DISCUSSION

The results of the char conversion experiments at atmospheric pressure are shown in Figure 2. Also shown on this figure are the theoretical conversions predicted using transfer parameters (X) calculated from the Kunii and Levenspiel (K&L)[5] and the Davidson and Harrison (D&H)[6] models. Reactivities determined from TGA tests (Table 1) were used in the theoretical conversion calculation. In both models, average bubble size was calculated from Mori and Wen[7] and the self-diffusion coefficient calculated as in Reference 8. Both theories overpredict the char conversion. Actual conversion corresponds to a mass-transfer parameter X = 0.75 as opposed to X = 1.79 predicted by K&L and X = 4.73 predicted by D&H, Table 2.

TABLE 2. MASS TRANSFER PARAMETER, X, FOR CHAR USED IN LABORATORY TESTS

Reactor Pressure, psia	U_o/U_{mf}	Kunii & Levenspiel	Davidson & Harrison	Experimental	Gas Diffusivity D_g (adjusted) cm^2/sec
14.7	9.34	1.79	4.73	0.75	0.52
70.0	3.78	1.99	5.78	0.08	0.0008

Examination of the expressions used to calculate X from both models reveals two parameters that can be adjusted to allow agreement between the experiment and the theory. These are the bubble diameter (D_B) and the gas self-diffusion coefficient (D_g). The bubble diameter would have to be adjusted to about 10 cm to allow X = 0.75. Since this is considerably larger than the reactor (D_T = 5.08 cm), it is necessary to adjust D_g. Adjusting D_g from a theoretical value of D_g = 3.33 cm^2/sec down to D_g = 0.52 cm^2/sec and using the Kunii and Levenspiel model results in X = 0.75 and agreement with the experimental data. The conversion results at 70 psia are shown in Figure 3. The experimentally determined X and D_g adjusted to achieve this X at 70 psia are shown in Table 2.

It is interesting to note that to achieve these low transfer parameters, models must be employed with more than one transfer resistance in series. One of the resistances must depend on gaseous diffusion. Figure 4 shows the comparison of mass-transfer parameters calculated using a simple resistance theory (D&H) and a three-resistance theory (K&L). In the D&H model, it is assumed that two transfer mechanisms are occurring in parallel. There is a macroscopic movement of gas from the bubble along with a microscopic diffusive transfer. As D_g goes to zero, the D&H model predicts that X approaches a finite value ($X \simeq 0.5$)^g dependent only on the macroscopic transfer between the bubble and particulate phase. Calculation as D_g goes to zero at the elevated pressures results in about the same value for X. Since this is substantially greater than the experimental X, a theory incorporating a totally diffusive resistance in series must be used.

The K&L theory assumes the same transfer mechanisms as D&H out of the bubble, but places a third resistance, namely the cloud, between the bubble and the particulate. The transfer through the cloud is only due to gaseous diffusion. Thus, for the K&L case, the diffusive transfer between the cloud and the particulate phase can choke off the flow and the overall coefficient between bubble and particulate can be adjusted as low as needed to agree with experiment.

SUMMARY OF RESULTS

1. A two-phase fluidized-bed model can be used to predict the conversion observed in the char-steam gasification reaction in a 5.08-cm fluidized-bed reactor.

2. The best fit of the experimental data was obtained using the K&L model to calculate the mass exchange between the bubble and particulate phases.

ACKNOWLEDGMENT

The work described in this paper was conducted under the sponsorship of the U.S. Department of Energy under Contract No. DE-AC21-78MC02798.

REFERENCES

1. Stewart, J. T. and Diehl, E. K., "Fluidized bed coal gasification - process and equipment development," Third International Conference on Fluidized Bed Combustion, Hueston Woods, Ohio, 1972. 19 pp.

2. Colaluca, M. A., Paisley, M. A., and Mahajan, K., "Development of the TRI-GAS gasification process," AIChE 71st Annual Meeting, Miami Beach, Florida, 1978. 27 pp.

3. Jenkins, R. G., Nandi, S. P. and Walker, P. L., Jr., "Reactivity of heat-treated coals in air at 500°C," Fuel 52, 288 (1973).

4. Orcutt, J. C., Davidson, J. F., and Pigford, R. L., "Reaction time distribution in fluidized catalytic reactors," AIChE Symposium Series 38, 58, 1 (1962).

5. Kunii, D. and Levenspiel, U., "Fluidization Engineering," New York: John Wiley & Sons, 1969. page 227.

6. Davidson, J. F. and Harrison, D., "Fluidized Particles," Cambridge: Cambridge University Press, 1963. page 98.

7. Mori, S. and Wen, C. Y., "Estimation of bubble diameter in gaseous fluidized beds," Fluidization Theories and Applications, AIChE Symposium Series 161, 73, 121 (1977).

8. Perry, R. M. and Chilton, C. H., "Chemical Engineers' Handbook," Fifth Edition, McGraw-Hill Book Co., 1973. page 3-230.

APPENDIX A

NOMENCLATURE

A_T = Reactor cross-sectional area, sq cm

C_O, C_P, C_B = Steam concentration in reactor inlet, particulate phase and bubble phase, moles/cu cm

D_g = Gas Diffusivity, sq cm/sec

D_T = Reactor diameter, cm

k = Reaction rate constant

L, L_{mf} = Fluid bed height, height at minimum fluidization, cm

M_C = Char molecular weight, gm/gm mole

n = Exponent for char reactivity

N = Number of bubbles per unit volume, 1/cu cm

N_C, N_R = Number of reacting moles of char and steam

Q = Effective volumetric flow rate from the bubble phase to the particulate phase, cu cm/sec

R_1, R_2, R_3, R_4, R_5 = Reactant transported from the bubble to particulate phase, fed to particulate phase, transported from the particulate to bubble phase, left the particulate phase and disappeared due to chemical reaction in particulate phase, moles/sec

S = Surface area of the rising bubble, sq cm

t, t_R = Time, solids residence time, sec

U_o, U_B, U_{mf} = Superficial velocity, bubble velocity, minimum fluidization velocity, cm/sec

V, V_P, V_{TMF} = Bubble volume, particulate phase gas volume, total fluid bed volume at minimum fluidization conditions, cu cm

W, W_o = Instantaneous char weight, weight at the instant the reacting gas is introduced (on ash-free basis), mg

X = Mass transfer parameter

y = Axial distance from the reactor inlet, cm

Y = W/W_o

α = Frequency factor

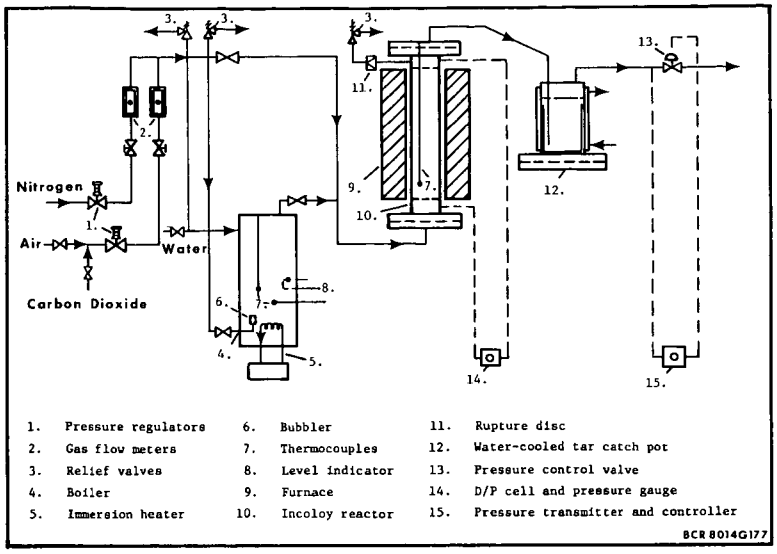

Figure 1. Flow Diagram of Laboratory Fluidized-bed Test Unit

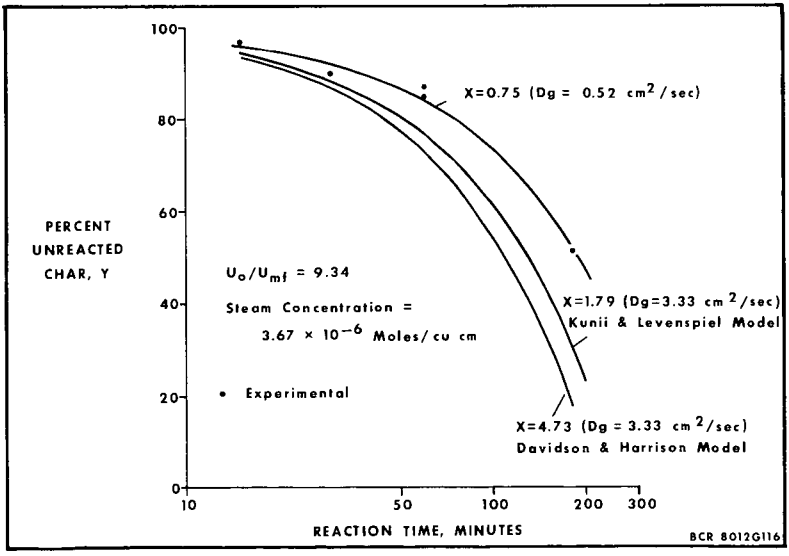

Figure 2. Char Conversion at Atmospheric Pressure and 1800°F Temperature

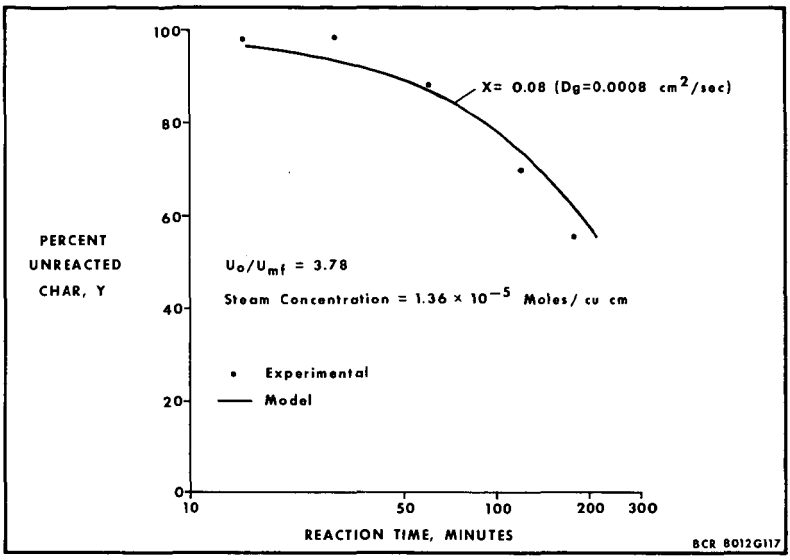

Figure 3. Char Conversion at 70 psia Pressure and 1800°F Temperature

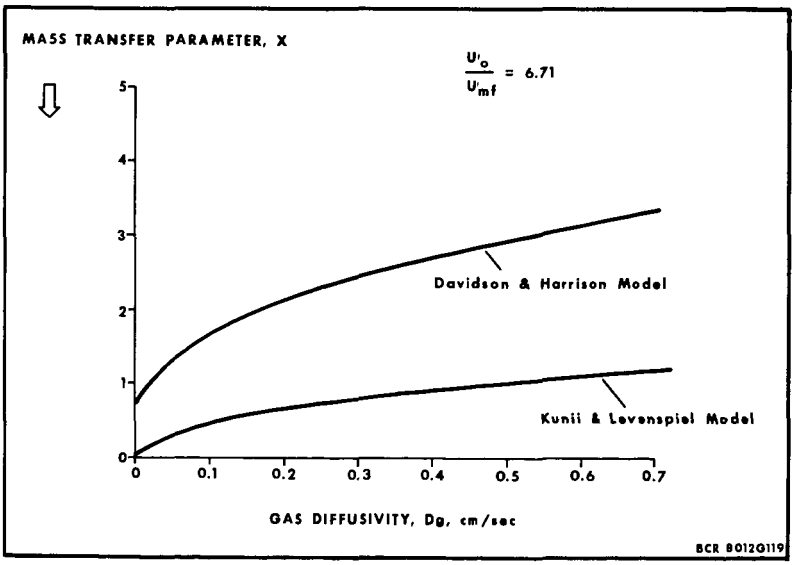

Figure 4. Diffusivity Effect on the Mass Transfer Parameter in a Fluidized-bed

ELECTROCHEMICAL ROUTE TO COAL GASIFICATION AND ITS TECHNOLOGICAL IMPLICATIONS

Robert W. Coughlin and M. Farooque

Department of Chemical Engineering
University of Connecticut
Storrs, CT 06268

Introduction

The production of synthetic natural gas or synthetic oil from coal consumes copious quantities of hydrogen that can be generated in large amounts only by processes which split the water molecule. Here we report on a new method for producing such hydrogen from coal, water and electric energy at mild temperatures. Conventional hydrothermal gasification of coal involves the well known steam-carbon reaction:

$$2C_{(s)} + H_2O_{(g)} \rightarrow 2CO_{(g)} + 2H_{2(g)} \quad 1)$$

and the water gas shift reaction:

$$CO_{(g)} + H_2O \rightarrow CO_{2(g)} + H_{2(g)} \quad 2)$$

To ensure favorable equilibrium reaction 1) is conducted at high temperatures. The chemistry and technology of such coal gasification are complex and a detailed discussion of such matters, including hardware and gasification equipment, has been published by Squires [1] and others [2-3].

We have reported [4] a newly developed electrochemical process which converts coal and water into two separate gaseous products, the one comprising essentially gaseous oxides of carbon and the other essentially pure hydrogen. The process chemistry takes place at mild temperatures (even room temperature) and the gaseous products are essentially free of impurities such as ash, tar and sulfur compounds. This new electrochemical gasification process involves the anodic oxidation of coal at an electrode for which we postulate the half-cell reaction of the carbon in coal:

$$C_{(s)} + 2H_2O_{(\ell)} \rightarrow CO_{2(g)} + 4H^+ + 4e^- \quad 3)$$

in combination with a corresponding half-cell reaction at the cathode:

$$4H^+ + 4e^- \rightarrow 2H_{2(g)} \quad 4)$$

The net sum of these half-cell reactions 3) and 4) is just the equation for the predominant reaction in the electrochemical gasification of coal:

$$C_{(s)} + 2H_2O_{(\ell)} \rightarrow 2H_{2(g)} + CO_{2(g)} \quad 5)$$

The application of an electrical potential and the input of electrical energy overcomes the free-energy barrier for reaction 5) at low temperatures and permits it to be accomplished even at room temperatures and actual practical potentials of about 0.85V - 1.0V. The thermodynamic reversible potential ($|\Delta G|/nF$) for equation 5) at room temperature is only 0.21V. A notable advantage of electrochemical gasification of coal over conventional methods of coal gasification is the production of gaseous oxides of carbon at the anode and the simultaneous production of essentially pure hydrogen separately at the cathode. Because each gaseous product is produced separately and essentially free of impurities such as sulfur, tar and ash, subsequent cleaning, separation and purification steps are minimized. Other manuscripts [4,5,6] have introduced the process of electrochemical coal gasification and reported initial data as to the reactivities of various coals, the effect of different operating conditions and variables, and distinguished the process from conventional water electrolysis. Its relationship to conventional methods of coal gasification and the well known steam carbon reaction was also discussed. In the present paper we present results obtained in galvanostatic and potentiostatic studies, and we also consider the

technological implication of this process in the field of H_2 production, and electrowinning of metals from aqueous electrolytes.

Experimental

All experiments were conducted with stirred slurries of coal in aqueous electrolyte within the anode compartment of a cell (details of the experimental apparatus are given in references [4,5]). The external emf was applied by a potentiostat (both Model PAR 371 and PAR 179A were used) and the electrodes (both anode and cathode) were Pt mesh, gauge 52 (0.004" diameter wire) supplied by Mathey Bishop, Inc.

Potentiostatic Studies: Effect of Potential and Course of the Reaction

The higher the potential the greater the oxidation current. As the coal is consumed by oxidation at a given potential the current diminishes very slowly. This behavior is shown in Figure 1 where current is plotted vs. potential for various extents of coal consumption* as a parameter. Similar behavior is evident in Figure 2, where observed reaction rates of three different coal samples and one activated charcoal at 1.0V, using a coal slurry concentration of 0.069 gm/cm^3 are plotted against cumulative coulombs passed. The results indicate that the rate of oxidation falls gradually as the reaction proceeds for all the samples studied. Only a portion (up to about 18% for NDL) of the coal can be consumed* before the rate of oxidation begins to fall steeply.

Previous workers [7-9] have reported that controlled oxidation of purer carbons, whether by electrochemical or chemical means results in the formation of several surface oxides. Of these oxides, the carboxylic group usually predominates. We believe, such oxides also form during the anodic oxidation of coal and they increase in concentration on the surface of the coal particles as the reaction advances, rendering electron abstraction more and more difficult, with consequent lowering of the oxidation current. Preliminary results obtained by analyzing the residual carbon values after partial electrochemical gasification of Pittsburgh coal also supports this view. Based on the known decomposition temperatures reported [10] for such surface oxygen compounds on carbon it should be possible to maintain a higher and steady oxidation rate at 200° - 600°C. It seems reasonable to consider surface oxides as intermediates in the pathway from coal and water as reactants to gaseous oxides of carbon and hydrogen as reaction products.

The decrease in oxidation current may also result in part from the accumulation on the coal particles of a tar-like coating that is formed during electrochemical coal gasification. Such a coating may be additional reaction products in the form of small aliphatic fragments which break away from larger coal molecules during anodic oxidation.

From Figure 2 it can be seen that the rate of oxidation of the Pittsburgh coal has dropped by a factor of about 7 when about 16% of the coal is electrochemically consumed. After it had been consumed to this extent, the coal was subjected to several treatments, to investigate the nature of the deactiviation and explore the possiblity of regeneration. The results disclose that the following treatments restore the original activity of the coal to a great extent: (A) washing with acetone which was also observed to remove tar-like material from the coal with the formation of a dark, perhaps colloidal, extract solution, and (B) heating in air to 250°C, which presumably removes accumulated

*Throughout this paper the extent of coal consumption is computed as the mass of carbon equivalent to total electrical charge passed during the experiment.

oxygen-containing surface functional groups [7]. In another experiment, North Dakota lignite was anodically oxidized at 1.0V and at 114°C with consumption of 26% of the coal, the remaining coal was filtered from the electrolyte, washed with acetone, and then heated in air to 250°C for 2 hours. This reactivated coal was then returned to the anolyte, and was further consumed an additional 20%. With the regenerated coal the oxidation current was almost equal to that observed with virgin coal and curve 2 of Figure 2 was essentially reproduced under the same conditions and with similar product formation. These experiments suggest that it would be possible to consume coal to a much larger extent at a meaningful rate by conducting the electrochemical gasification reaction at temperatures of about 200°C and above. Experiments at higher temperatures are planned and will be reported in another paper.

Galvanostatic Studies: Effect on the Cell Potential

North Dakota lignite was electrochemically gasified under galvanostatic conditions. Initially, the fresh coal samples were oxidized at a constant oxidation current of 150 mA until 9.82% of the coal was consumed, then the oxidation rate was lowered to 100 mA. The corresponding change of cell potential is plotted against the percentage of the total coal consumed in the process in Figure 3. The results clearly indicate that to maintain the desired rate of the reaction, the cell potential gradually rises because, as explained above, the coal particles become more and more unreactive as the reaction progresses (there may also be some effect due to decreasing coal concentration as well.) The potential required to maintain a constant current of 150 mA continues to rise in Figure 3 to about 1.2V (attained at first after about 97 hr) whereupon the required potential rises abruptly to about 1.7V, thereby suggesting the onset of a different reaction mechanism. As evident in Figure 3 this discontinuity at 1.2V was reproducible at two different currents (150mA and 100mA) and two corresponding different stages of coal consumption. It should be noted that analysis of the anode gas revealed only CO_2 and CO and no trace of O_2 until the potential reached 1.98V. It appears, therefore, that the discontinuity at 1.2V may correspond to the onset of a different mechanism of electrochemical coal gasification; it cannot be explained as the onset of simple water electrolysis.

Temperature Effects

It is suggested above that it would be possible to consume coal to a much larger extent at a meaningful rate by conducting the electrochemical gasification reaction at temperatures of about 200°C and above. Higher temperature operations may also provide other benefits:

(i) polarization potentials (overvoltages) would be lowered and
(ii) the reversible (thermodynamic) cell potential would also be lowered as explained below.

Figure 4 shows the effect of temperature on the reversible cell potential as computed from the thermodynamic ΔG and ΔH values of the electrochemical coal gasification reaction 5). Referring to this figure, the electrochemical coal gasification cannot occur below the reversible thermodynamic potential that corresponds to the Gibbs free energy of reaction (ΔG); this voltage decreases with increasing temperature. It is possible in principle for electrolysis to occur at any potential above the reversible thermodynamic value, if $T\Delta S$ is supplied as heat from the surroundings, but in practice polarization effects and other irreversibilities require larger potentials in order to operate at reasonable rates of reaction.

If the cell is operated at or above the thermoneutral voltage

$(= \frac{|\Delta H|}{nF})$ both ΔG and $T\Delta S$ are supplied as electrical energy and no additional energy is required because the entire endothermic heat of reaction is supplied as electrical energy. Above the thermoneutral voltage there would be net heat generation and heat removal would be necessary.

Gases Produced and the Current Efficiency

During the oxidation of NDL, Pittsburgh coal, activated carbon and Montana Rosebud char at potentials between 0.8V to 1.2V the gas produced at the cathode was essentially pure H_2 and in each case the current efficiency of H_2 production was around 100% based on measured current integrated over time. The gas produced within the anode compartment was almost pure CO_2 with small amounts of CO. The composition of the anode gas, however, varies somewhat over the course of the gasification reaction; this may be attributed to corresponding changes in population of surface oxides on the coal. It is also observed that the volume ratio of the gases collected at the cathode to those at the anode ranged from about 9.1 to 3.7; the higher ratios were obtained at the beginning of the experiment but then decreasesd. According to the stoichiometry of reaction 5) this gas ratio should be about 2. Cathode-to-anode gas ratios greater than about 2.0 can be attributed mainly to accumulation of oxygen on the coal particles in the form of functional groups such as -COOH, -CHO, CH_2OH and the like. Moreover, higher relative amounts of H_2 may also be attributed in part as arising from the hydrogen content of the coal. Preliminary proximate analysis of the residual carbon after NDL gasification reveals preferential consumption of volatile components which are expected to be rich in hydrogen. The production of anode gas is probably strongly related to the concentration of the surface oxides of coal. Binder et al reported [7] that a surface layer forms first on graphite and only then does CO_2 evolution begin. As the oxidation process advance, surface oxides may build up to steady-state concentrations on the coal, whereupon the anode compartment gas generation rate becomes constant. A qualitative but sensitive mass spectrometric analysis was made of the gases produced at both anode and cathode. It is noteworthy that no lines were observed for molecular weights corresponding to SO_2 or H_2S--even though the parent coals contain significant sulfur.

Implications for Hydrogen Production

The more common approaches to splitting the water molecule to recover hydrogen have utilized either electrical energy alone or fossil fuel in combination with thermal energy. It appears that the production of hydrogen by the combined use of fossil fuel and electrical energy as we report has not previously been investigated or applied. In the following the efficiency of H_2 production by our new process("Coal-Consuming Water Electrolysis") is compared with ordinary water electrolysis. In water electrolysis the energy required to split the water molecule is supplied solely by electricity, whereas in our new process the required energy is supplied only in part by electricity with the balance arising by way of the concomitant anodic oxidation of coal. The following quantitative development gives a first order approximation of how much energy comes from each such source and thereby provides a rough feeling for efficiency. The energy consumed by conventional water electrolysis conducted at a potential of E_2 to produce N_{H_2} moles of H_2 is $2N_{H_2}$ F E_2 whereas the energy required by the present process under investigation operating at a potential of E is:

$$E\int_0^t i\,dt + N_c(-\Delta H) \qquad 6)$$

where E is the potential applied across the cell, i is the current and

t is time. N_c is the number of moles of carbon consumed and ΔH is the enthalpy of combustion of carbon to CO_2.

The foregoing expression can be simplified by assuming a constant operating potential E, and noting that:

$$N_{H_2} = \int_0^t i dt/2F \qquad 7)$$

and $$N_c = 1/2\ N_{H_2} \qquad 8)$$

where F, the Faraday constant, is 96,500 coulombs/equivalent.

Eliminating $\int_0^t i dt$ and N_c the expression for total energy consumption by our process becomes:

$$2FN_{H_2}E + 1/2\ N_{H_2}\ (-\Delta H) \qquad 9)$$

The relative energy usage (REU) is accordingly:

$$REU\left(\frac{\text{Ordinary Electrolysis}}{\text{Coal Assisted Electrolysis}}\right) = \frac{2N_{H_2}F\ E_2}{2F\ N_{H_2}E + 1/2\ N_{H_2}|\Delta H|} \qquad 10)$$

$$= E_2/(E + |\Delta H|/4F)$$

Inserting $|\Delta H|$ = 94,100 x 4.18 joules/mole and the value of F gives:

$$REU = E_2/(E + 1.02) \qquad 11)$$

Practical values of E_2 for conventional electrolysis are about 1.8-2.0V whereas values of E observed in the present work have ranged from about 0.8 to about 1.0 volt at room temperature. This means that, per unit of hydrogen produced, the total energy consumption is about the same (REU ≃ 1) for ordinary water electrolysis and for coal-assisted water electrolysis conducted in the experiments near room temperature reported here. In the case of electrochemical gasification to hydrogen, however, about half the required energy comes directly from coal and half from electricity. We expect that the total energy requirement for coal-assisted water electrolysis can be lowered further by conducting it at higher temperatures thereby permitting operation at lower potentials (E) than 0.8 - 1.0 volt. A detailed economic analysis reported elsewhere [5] shows that coal-assisted electrolysis has its most favorable effect when electricity costs are high because cheaper coal energy is substituted for more costly electrical energy. The greatest effect (a 27% reduction in hydrogen cost) is evident for application with SPE technology at "normal" power costs of $0.027/kw.hr.: the corresponding cost reduction for conventional electrolysis is 18%. For off-peak power at $0.01/kw.hr. it is seen that direct incorporation of coal into the electrolysis process seems to offer no particular advantage.

Implications for Electrowinning of Metals

Electrochemical coal gasification can be extended to the electrowinning of metals by substituting the half cell reaction 3) (which consumes coal) for the half-cell reaction of oxygen evolution which ordinarily takes place during conventional electrowinning of metals from aqueous solutions of their salts. By this coal-based innovation the total overall cell potential of the resulting metal electrowinning process is lowered by about 1.10V with a corresponding significant reduction in the consumption of electrical energy. As a test case Cu was deposited on a platinum mesh cathode (separated from the anode by a fritted glass barrier) from aqueous electrolyte (0.125 M $CuSO_4$ in 0.5 M H_2SO_4) at 60°C, at two different galvanostatic rates; 5.9 mA and 12 mA. The corresponding change in cell potential is plotted in Figure 5. It is evident that the conventional copper electrowinning

reactions took place at cell potentials of about 1.65V and 1.73V respectively. Also plotted in Figure 5 are the results obtained in parallel experiments conducted in identical fashion except that the coal was simultaneously oxidized at the anode according to equation 3) while Cu cations were reduced at the cathode. In these latter experiments, North Dakota lignite (NDL) coal slurry (0.15 gm/cm^3) was introduced into the anode compartment of the cell and was anodically oxidized while copper deposited on the cathode under identical galvanostatic experimental conditions. As a result of the oxidation or gasification of the coal at the anode, the overall cell potential was lowered by about 1.1V, compared to the conventional process. This is evident from the comparative data plotted in Figure 5.

Concluding Remarks

It has been shown in this study that

(i) different coals have different reactivities for electrochemical gasification and in each case the reactivity of the particular coal falls gradually as the reaction advances.

(ii) the original reactivity of the coal samples can be restored by acetone washing and heating at temperatures between 200° - 600°C.

(iii) high temperature operation promises several advantages.

(iv) two different coal oxidation mechanisms appear to occur in two correspondingly different potential regions of oxidation.

(v) hydrogen production and electrowinning of metals from aqueous electrolytes are the processes where electrochemical coal gasification may find application.

Mass balance calculations, high temperature reaction and use of anodes other than platinum are currently in progress.

Acknowledgement

We are grateful for the financial support of this research by the University of Connecticut Research Foundation and the U.S. Department of Energy. Valuable experimental assistance was provided by Larry Veneziano.

References

1. A. M. Squires, Science 184, 340-46 (1974).
2. G. E. Klingman and R. P. Schaaf, Hydrocarbon processing, pp. 97-101 (April 1972).
3. A. Verma, Chem. Tech; 372-81, June (1978).
4. R. W. Coughlin and M. Farooque, Nature (accepted for publication).
5. R. W. Coughlin and M. Farooque, IC & E (submitted).
6. M. Farooque and R. W. Coughlin, Fuels (submitted).
7. H. Binder, A. Köhling, K. Richter and G. Sundstede, Electrochimica Acta, 1964, Vol. 9, 255 (1964).
8. R. E. Panzer and P. J. Elving, Electrochimica Acta, Vol. 20, 635 (1975).
9. R. W. Coughlin, Ind. Eng. Chem. Prod. R & D 8, 12 (1969).
10. Y. A. Zarifyanz, V. F. Kiseleve, N. N. Lezhnev and D. V. Nikitina, Carbon 5, 127 (1967).

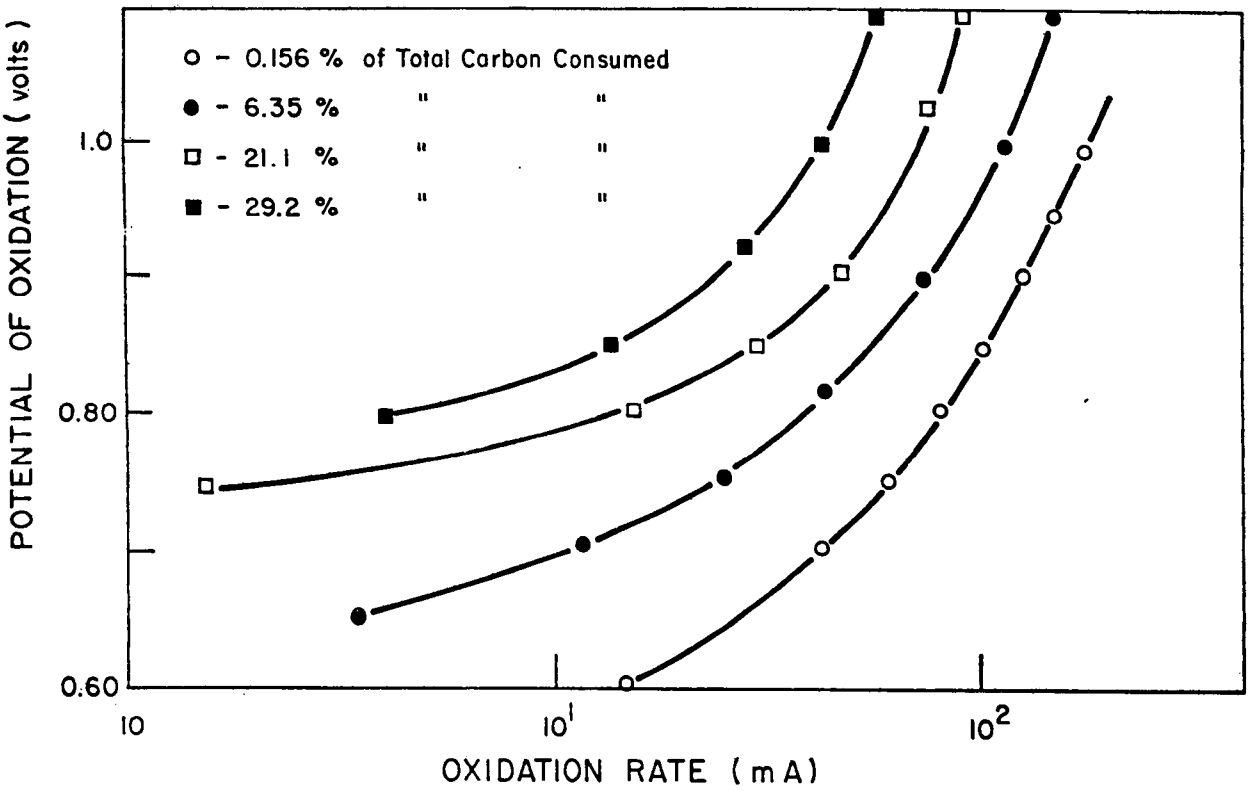

1. Effect of Potential on the Oxidation Rate as the Reaction Proceeds.

(North Dakota Lignite; Coal Slurry Conc.: 0.069 gm/cm^3; Supporting Electrolyte: 5.60 M H_2SO_4; Particle Size: 125 - 149μm, Temp. 114°C; Anode area: 96.5 cm^2 (geometrical).

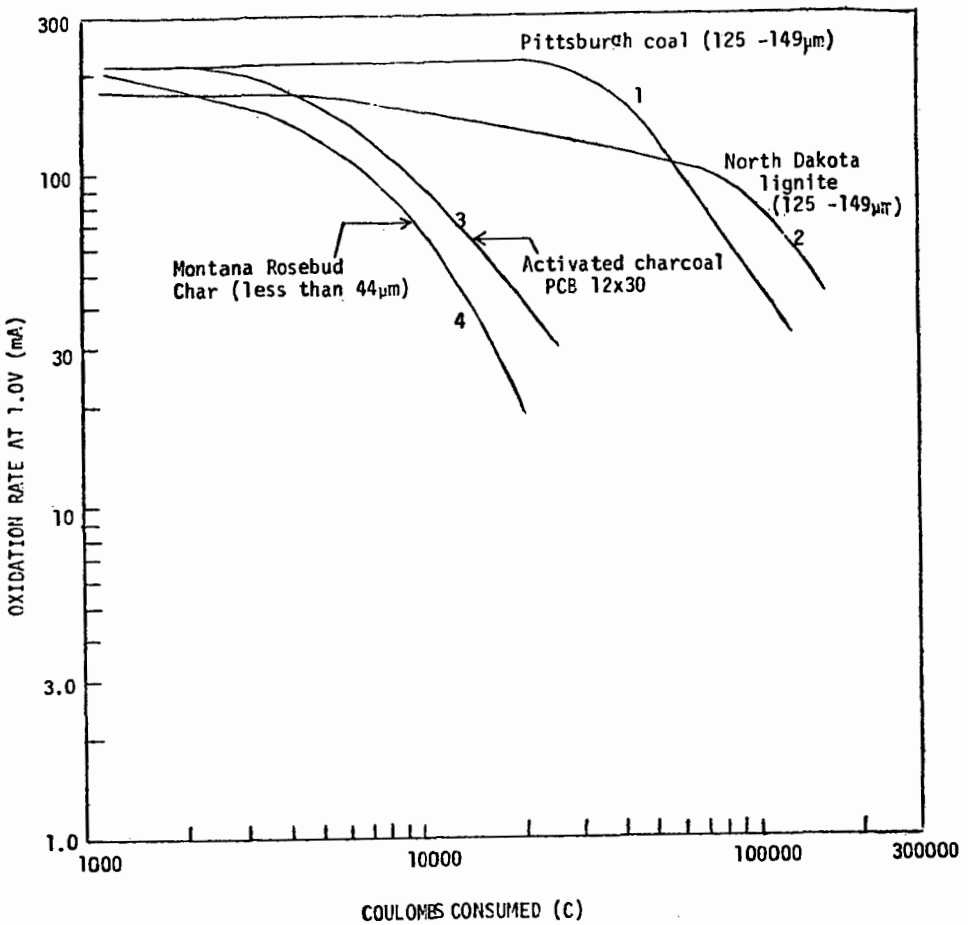

2. Oxidation Rate of Different Samples At 1.0V as the Reaction Proceeds.

(Slurry Conc.: 0.069 gm/cm^3; Particle Size: 44μm and below; Electrolyte: 5.6M H_2SO_4; Potential: 1.0V; Anode area: 96.5 cm^2 (geometrical); Temp. 114°C.

Electrolysis discontinued after:
Curve 1: 343 hours and 16.36% consumed
Curve 2: 353 hours and 29.2% consumed
Curve 3: 110 hours and about 2.56% consumed
Curve 4: 78 hours and 3.2% consumed

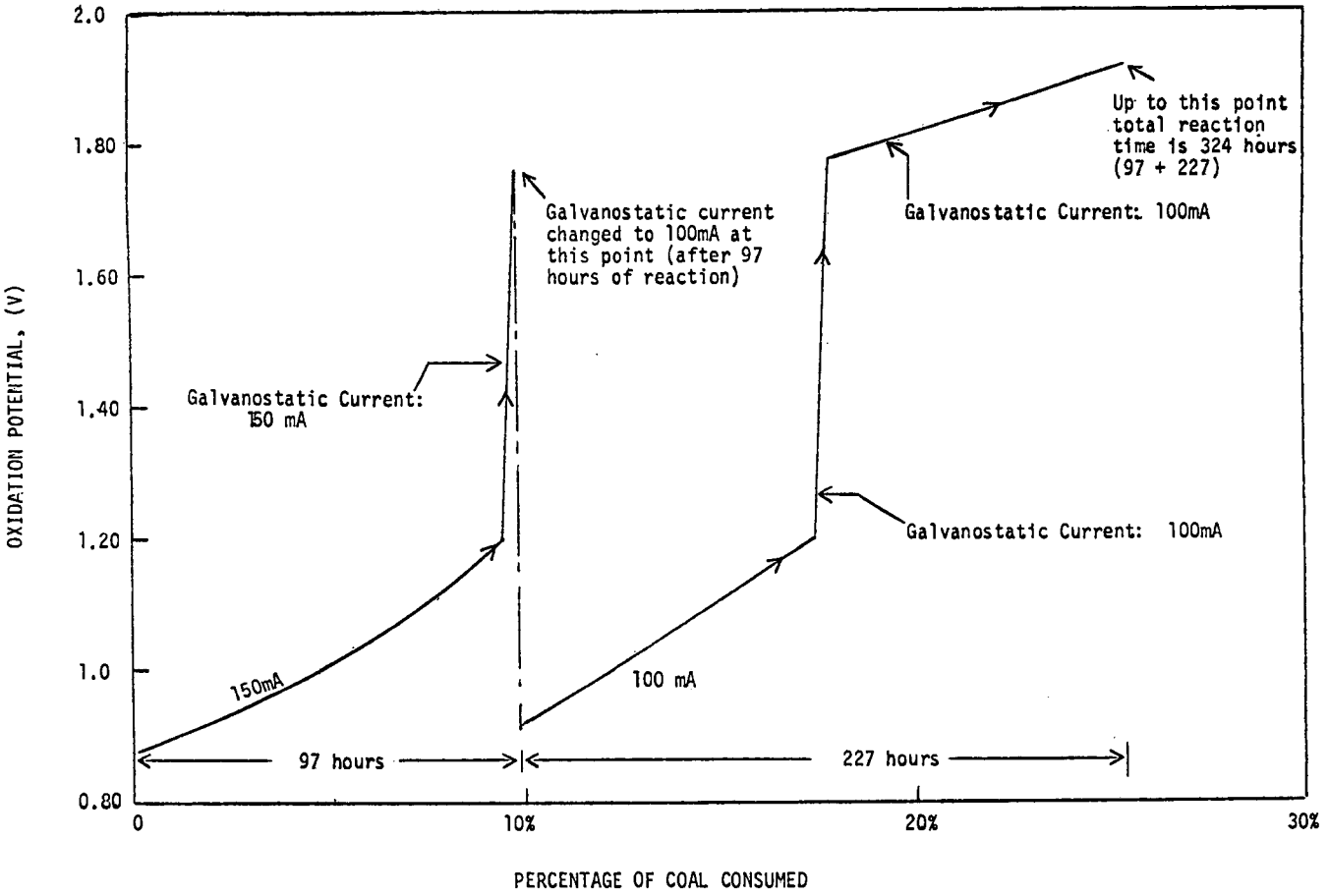

Figure 3. Change of Cell Potential During Galvanostatic Study.

(Coal sample: Fresh NDL; Slurry Conc.: 0.069 gm/cm^3;
Electrolyte: 5.6M H_2SO_4; Particle size: 105-125μm;
Anode area: 96.5 cm^2 (geometrical).

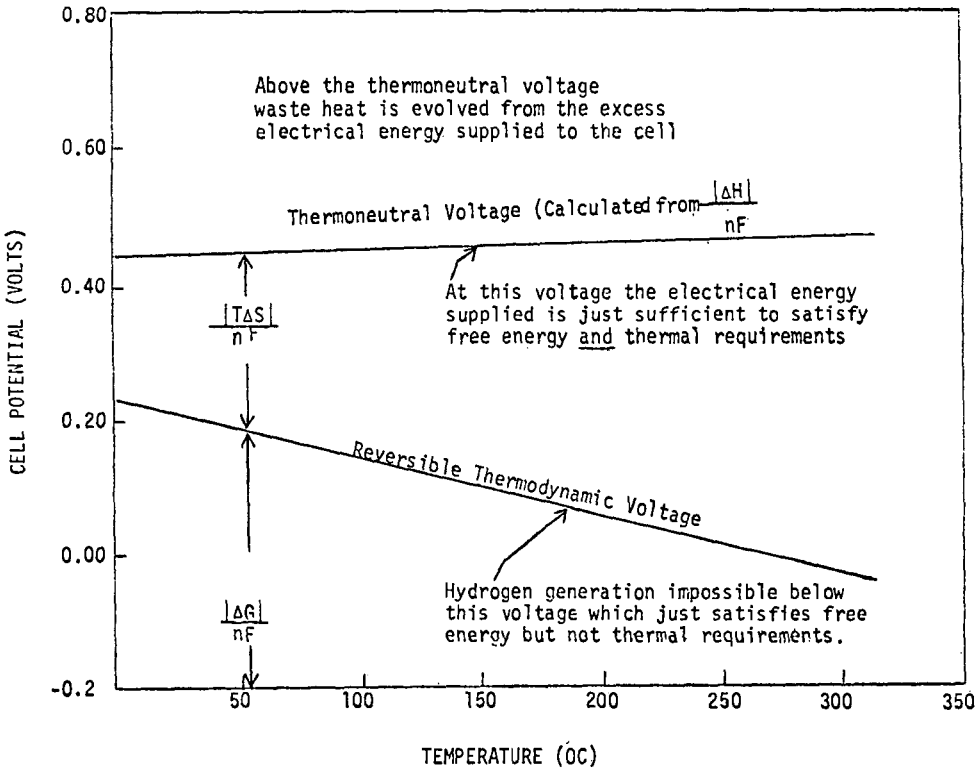

Figure 4. Effect of Operating Temperature on Cell Voltage.

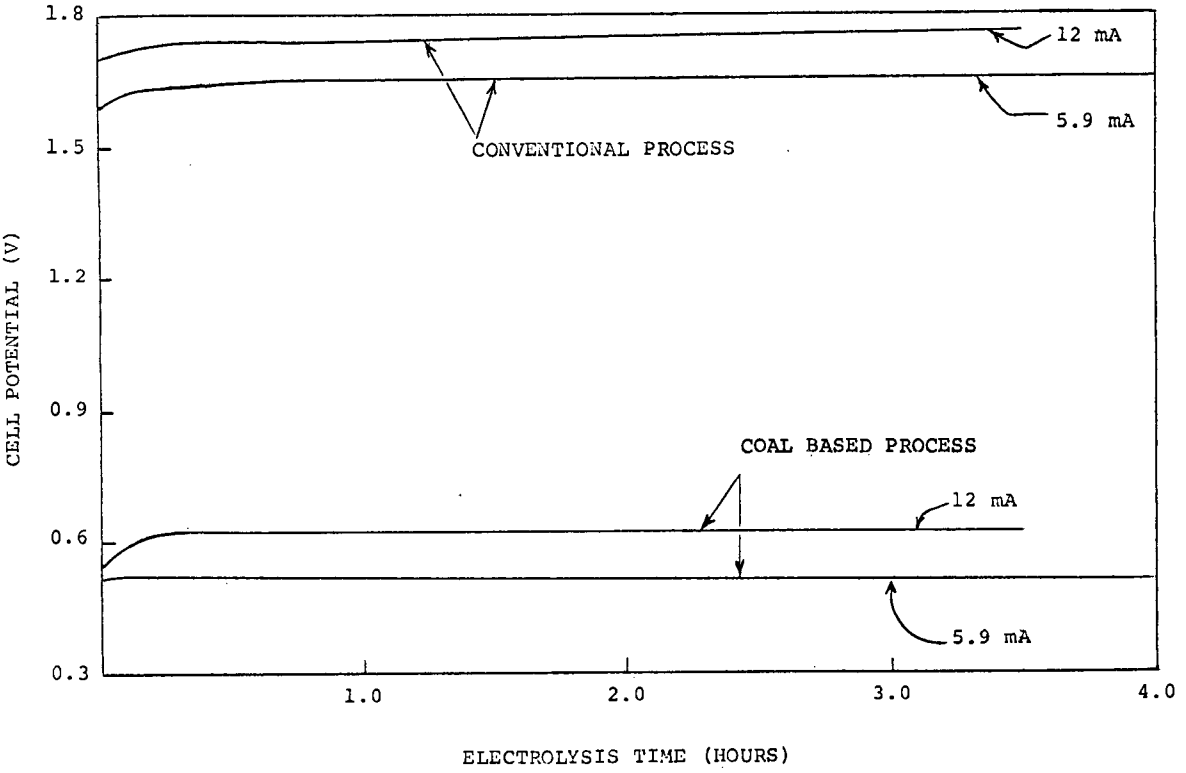

Figure 5. Comparison of the Cell Potentials of the Conventional and and Coal Based Copper Electrowinning Processes.

(Electrolyte: 0.125M $CuSO_4$ and 0.5M H_2SO_4; Coal Sample N. Dakota Lignite; Slurry Conc.: 0.15gm/cm^3; Particle size: 74-88μm; Temp.: 60°C; Anode area: 5.3 cm^2 (geometrical).